

**OPTIMIZATION OF SATELLITE TRANSPONDER UTILIZATION
BASED ON SIMULATION RESULTS**

A MASTER'S THESIS

in

Electrical and Electronics Engineering

Atilim University

by

ORHAN ULUBEY

JANUARY 2015

**OPTIMIZATION OF SATELLITE TRANSPONDER UTILIZATION
BASED ON SIMULATION RESULTS**

**A THESIS SUBMITTED TO
THE GRADUATE SCHOOL OF NATURAL AND APPLIED SCIENCES
OF
ATILIM UNIVERSITY**

**BY
ORHAN ULUBEY**

**IN PARTIAL FULFILLMENT OF THE REQUIREMENTS FOR THE
DEGREE OF**

MASTER OF SCIENCE

IN

**THE DEPARTMENT OF ELECTRICAL AND ELECTRONICS
ENGINEERING**

JANUARY 2015

Approval of the Graduate School of Natural and Applied Sciences, Atılım University.

Prof. Dr. İbrahim AKMAN

Director

I certify that this thesis satisfies all the requirements as a thesis for the degree of Master of Science.

Assoc. Prof. Dr. Elif AYDIN

Head of Department

This is to certify that we have read the thesis “Optimization of Satellite Transponder Utilization Based on Simulation Results” submitted by “Orhan ULUBEY” and that in our opinion it is fully adequate, in scope and quality, as a thesis for the degree of Master of Science.

Assoc. Prof. Dr. Ali KARA

Supervisor

Examining Committee Members

Assoc. Prof. Dr. Ahmet Fazıl YAĞLI

Asst. Prof. Dr. Ahmet PAKFİLİZ

Asst. Prof. Dr. İ. Baran USLU

Dr. İbrahim ÖZ

Assoc. Prof. Dr. Ali KARA

Date: 30.01.2015

I declare and guarantee that all data, knowledge and information in this document has been obtained, processed and presented in accordance with academic rules and ethical conduct. Based on these rules and conduct, I have fully cited and referenced all material and results that are not original to this work.

Orhan ULUBEY

Signature:

ABSTRACT

OPTIMIZATION OF SATELLITE TRANSPONDER UTILIZATION BASED ON SIMULATION RESULTS

Ulubey, Orhan

M.S., Electrical and Electronics Engineering Department

Supervisor: Assoc.Prof.Dr. Ali KARA

January 2015, 64 pages

Communication satellite transponder performance is characterized through the manufacturing process with extensive tests. However, such performance tests are always carried out with unmodulated carriers and they have shortcomings when it is necessary to analyze the transponder behavior with modulated multicarrier scenarios faced in actual utilization of the satellite. To overcome this problem it is necessary to simulate the behavior of transponder and obtain results to aid in link budget calculations. This thesis reviews the communication impairment sources on a satellite transponder and introduces a transponder simulator based on TURKSAT-3A satellite measured data. Simulation results are used to characterize the degradation introduced by the transponder for various actual utilization scenarios and suggestions made for optimal use.

Keywords: Communication satellite, Transponder simulation, Total Degradation, Transponder linearity, Multicarrier.

ÖZ

SİMÜLASYON SONUÇLARINA GÖRE UYDU AKTARICI KULLANIM OPTİMİZASYONU

Ulubey, Orhan

Yüksek Lisans, Elektrik Elektronik Mühendisliği Bölümü

Tez Yöneticisi: Doç. Dr. Ali KARA

Ocak 2015, 64 sayfa

Haberleşme uyduları aktarıcı performansı üretim sürecindeki yoğun testler ile karakterize edilir. Bununla birlikte, aktarıcının gerçek kullanımına uygun olarak modüle edilmiş çoklu taşıyıcı senaryolarındaki davranışı analiz edilmek istenildiğinde, üretim sürecinde modüle edilmemiş taşıyıcılar ile uygulanan bu test sonuçları yetersiz kalmaktadır. Bu sorunun çözümü için aktarıcı davranışı modellenerek, link bütçesi hesaplarına yardımcı olacak sonuçlar elde edilmelidir. Bu tezde, uydu aktarıcısında haberleşme sinyallerine bozucu etkide bulunan kaynaklar incelenmekte ve TÜRKSAT-3A uydusunun test verisi kullanılarak hazırlanmış bir aktarıcı simülatörü tanıtılmaktadır. Simülasyon sonuçları aktarıcının gerçek kullanım senaryolarında neden olduğu toplam bozulma etkisini karakterize etmek ve buna dayalı olarak optimum kullanım önerileri getirmek için kullanılmıştır.

Anahtar Kelimeler: Haberleşme uydusu, Aktarıcı simülasyonu, Toplam bozulma, Aktarıcı doğrusallığı, Çoklu taşıyıcı.

GCCRIIS

To My Family

ACKNOWLEDGEMENTS

I express sincere appreciation to my supervisor Assoc. Prof. Dr. Ali KARA for his guidance and criticism throughout the research. To my wife, kids and whole family, I offer sincere thanks for their continuous support and patience during this period.

TABLE OF CONTENTS

ABSTRACT	iii
ÖZ	iv
ACKNOWLEDGEMENTS	vi
TABLE OF CONTENTS	vii
LIST OF TABLES	ix
LIST OF FIGURES	x
CHAPTER 1	1
INTRODUCTION	1
CHAPTER 2	3
SATELLITE TRANSPONDER STRUCTURE AND SOURCES OF COMMUNICATION IMPAIRMENT	3
2.1. Transponder Structure.....	3
2.2. Communication Impairments	7
2.2.1. AM/AM and AM/PM Transfer Curves	7
2.2.2. Intermodulation (IM)	9
2.2.3. Noise Power Ratio (NPR)	12
2.2.4. Filters' Amplitude and Group Delay Responses	14
CHAPTER 3	16
SIMULATION SYSTEM MODEL.....	16
3.1. Transponder Model	17
3.2. Transmission Model.....	21
3.2.1. Carriers.....	21

3.2.2. Modulations.....	22
3.2.3. Transmit Filter	24
3.2.4. Uplink Signal Simulation.....	25
3.3. Receiver Model.....	27
CHAPTER 4.....	30
TOTAL DEGRADATION ANALYSIS.....	30
CHAPTER 5.....	33
RESULTS AND DISCUSSION.....	33
5.1. Single QPSK Modulated Carrier.....	33
5.2. Dual QPSK Modulated Carriers	35
5.3. Multicarrier Scenario with 8 QPSK Modulated Carriers	36
5.4. Single Carrier Scenario with Various Modulations	39
5.5. Link Budget Calculations and Optimization of Transponder Utilization	43
5.5.1. Dual Carrier Scenario Link Budget Calculations.....	45
5.5.2. Multicarrier Scenario with 8 QPSK Modulated Carriers Link Budget Calculations	50
5.5.3. Evaluation of Link Budget Calculations.....	52
CHAPTER 6.....	53
CONCLUSIONS	53
REFERENCES.....	56
APPENDIX A	59
SATELLITE LINK BUDGET CALCULATION	59
APPENDIX B.....	62
SIMULATION OUTPUT EXAMPLES	62

LIST OF TABLES

TABLE

Table 1 Simulated Carrier Scenarios	21
Table 2 Optimum Operation Points wrt. Modulation for Simulated LTWT	41
Table 3 Comparison of Simulated Performance with a Manufacturer's Data	42
Table 4 Optimum Performance Comparison for Dual Carrier Scenario	49
Table 5 Link Budget Calculation – Inputs	59
Table 6 Link Budget Calculation – Outputs 1/2.....	60
Table 7 Link Budget Calculation – Outputs 2/2.....	61

LIST OF FIGURES

FIGURES

Figure 1 Simplified Transparent Repeater Block Diagram.....	3
Figure 2 Normalized characteristics of TWT as a function of IBO (a) P_{in} - P_{out} or AM/AM curve (b) Gain Variation (c) Relative Phase Shift or AM/PM curve	8
Figure 3 AM/AM and AM/PM responses of a T3A TWT and associated LTWT	9
Figure 4 Normalized power transfer characteristics with two unmodulated carriers .	10
Figure 5 C/IM3 performance of a T3A TWT and associated LTWT	12
Figure 6 NPR Measurement	13
Figure 7 NPR performance of a T3A LTWT	13
Figure 8 Amplitude and Group Delay responses of a T3A OMUX Channel	14
Figure 9 Simulation Transponder Model	17
Figure 10 T3A OMUX filter (a) constructed magnitude response (b) measured magnitude response.....	19
Figure 11 T3A OMUX filter (a) constructed group delay response (b) measured group delay response.....	19
Figure 12 Simulated Carrier Placements over the 36 MHz Transponder	22
Figure 13 QPSK and 8PSK modulations, AWGN linear channel.....	23
Figure 14 16APSK and 32APSK modulations, AWGN linear channel	24
Figure 15 64APSK and 256APSK modulations, AWGN linear channel	24
Figure 16 Impulse Response of Transmit SQRC Filter	25
Figure 17 Comparison of Theoretical BER with SA and MC Simulated BER	29
Figure 18 (a) PSD of carrier at OMUX out (b) Constellation (c) BER vs E_b/N_0	32
Figure 19 Total Degradation for 30Msps Single Carrier with TWT	34
Figure 20 Total Degradation for 30Msps Single Carrier with LTWT.....	34
Figure 21 Total Degradation for a single carrier with varying symbol rate.....	35
Figure 22 Total Degradation for dual 14.8 Msps carriers	36
Figure 23 Total Degradation for multicarrier scenario with 8 carriers	37

Figure 24 ACI analysis for two 3.5Msps carriers with varying separation (a) $\Delta f=4.2$ MHz, (b) $\Delta f=3.85$ MHz, (c) $\Delta f=3.5$ MHz,.....	38
Figure 25 ACI analysis degradation curve	38
Figure 26 Uncoded AWGN BER Performances of 8PSK and M-APSK Modulations	40
Figure 27 Degradation (Δ) for QPSK, 8PSK, 16APSK and 32APSK Modulations ..	41
Figure 28 TD and 60cm Antenna Link Margin for Dual Carrier Scenario	47
Figure 29 Link Margin for Dual Carrier Scenario – 60cm and 2.4m Rx Antennas ...	48
Figure 30 Link Margin Comparison for Dual Carrier Scenario – TD, C/IM3 and NPR	50
Figure 31 Link Margin Comparison for 8 Carriers Scenario – TD, C/IM3 and NPR	51
Figure 32 Power Spectral Density Plots of Single Carrier, LTWT at -2dB IBO	62
Figure 33 Power Spectral Density Plots of Dual Carriers, LTWT at -2dB IBO	63
Figure 34 Power Spectral Density Plots of 8 Carriers, LTWT at -2dB IBO	64

LIST OF ABBREVIATIONS

ACI	-	Adjacent Channel Interference
AM/AM	-	Amplitude to Amplitude Modulation
AM/PM	-	Amplitude to Phase Modulation
ASI	-	Adjacent Satellite Interference
AWGN	-	Additive White Gaussian Noise
BER	-	Bit Error Rate
bps	-	bits per second
C Band	-	6 GHz U/L; 4 GHz D/L frequency band (typical)
C/I	-	Carrier to Intermodulation Ratio
C/IM3	-	Carrier to third order intermodulation ratio
CW	-	Continuous Wave
D/C	-	Down Converter
D/L	-	Downlink
dB	-	Decibel
DTH	-	Direct to Home (TV transmission)
DVB-S/S2/S2X	-	Digital Video Broadcasting – Satellite/ 2 nd Generation/ 2 nd Generation Extension
E_b/N_0	-	Energy per bit to noise power spectral density ratio
EIRP	-	Equivalent Isotropically Radiated Power
E_s/N_0	-	Energy per symbol to noise power spectral density ratio
FDM	-	Frequency Division Multiplexing
FEC	-	Forward Error Coding

FIR	-	Finite Impulse Response
G/T	-	Gain to Noise Temperature Ratio
HPA	-	High Power Amplifier
HTS	-	High Throughput Satellite
IBO	-	Input Back-off
IM	-	Intermodulation
IMUX	-	Input Multiplexer
ISI	-	Inter Symbol Interference
ITU	-	International Telecommunication Union
Ka Band	-	27-31 GHz U/L; 17-21 GHz D/L frequency band (typical)
Ku Band	-	14 GHz U/L; 11-12 GHz D/L frequency band (typical)
L Band	-	1.6 GHz U/L; 1.5 GHz D/L frequency band (typical)
LM	-	Link Margin
LNA	-	Low Noise Amplifier
LTWT	-	Linearized Travelling Wave Tube Amplifier
M-APSK	-	M-ary Amplitude and Phase Shift Keying
MC	-	Monte Carlo
MMIC	-	Monolithic Microwave Integrated Circuit
M-PSK	-	M-ary Phase Shift Keying
Mps	-	Mega symbols per second
NPR	-	Noise Power Ratio
OBO	-	Output Back-off
OMUX	-	Output Multiplexer
PSD	-	Power Spectral Density

QPSK	-	Quadrature Phase Shift Keying
Rx	-	Receive
S Band	-	2.6 GHz U/L; 2.5 GHz D/L frequency band (typical)
SA	-	Semianalytic
SER	-	Symbol Error Rate
SQRC	-	Square root Raised Cosine
SSPA	-	Solid State Power Amplifier
T3A	-	TURKSAT-3A Communication Satellite
TD	-	Total Degradation
TWT	-	Travelling Wave Tube
TWTA	-	Travelling Wave Tube Amplifier
Tx	-	Transmit
U/L	-	Uplink
VSAT	-	Very Small Aperture Terminal
XPI	-	Cross Polarization Interference

CHAPTER 1

INTRODUCTION

Satellite operators are competing with each other to be able to provide the most cost effective solution to their customers and on top of it, they rival terrestrial operators. When the high cost of satellites and related earth station equipment added into the equation, satellite operators have very challenging market conditions. Therefore, for a satellite operator, having the ability to analyze end to end link performance as precise as possible for both existing and planned communication satellites is inevitable in order to have a correct judgment about current and future assets.

Current satellite transmissions widely incorporate DVB-S and S2 standards for both TV and data applications. Since the first release of DVB-S in 1994, following the needs and advances in satellite communication industry, the DVB standard evolved accordingly and draft version of DVB-S2X has recently been released [1], [2]. While DVB-S has foreseen the use of only QPSK, 8PSK and 16 QAM waveforms, DVB-S2 brought in 16APSK and 32APSK. Ultimately, DVB-S2X extension defines 64, 128 and 256APSK modulations. Although, QPSK and 8PSK are still the most widespread modulations used for Direct-to-home (DTH) TV transmissions in a single carrier per transponder basis, high throughput satellite applications are benefiting from the efficiency improvements of 16APSK and 32APSK waveforms in the forward link and multicarrier scenarios are prevailing. It is evident that the race for higher efficiency figures will continue in parallel with the rising demand for broadband access. On the other hand, unlike the evolution of waveforms used in modern satellite communications, the performance specifications of satellite payload subsystems and the tests applied in manufacturing process to characterize the payload have almost stayed the same. $C/IM3$ (carrier to 3rd order intermodulation ratio) performed with two unmodulated carriers and NPR (noise power ratio) measurements, for instance, are still the performance metrics for evaluating the linearity performance albeit they are not fully capable of characterizing multicarrier high order digital modulation scenarios.

Given the necessity of precise end to end performance characterization and the shortcomings of available test data from manufacturing process, the conclusion is the need for reliable transponder simulations constructed upon actual test data to assist link budget calculations. The simulator shall handle TWT (travelling wave tube) AM/AM (amplitude to amplitude modulation) and AM/PM (amplitude to phase modulation) nonlinearities and degradation introduced by IMUX (input multiplexer) and OMUX (output multiplexer) filters' magnitude and group delay responses for given digital modulated carrier scenarios. Eventually, total degradation (TD) composed of impairments like intermodulation (IM) distortion, adjacent channel interference (ACI) and inter symbol interference (ISI) resulting from aforementioned nonlinearities and filtering has to be characterized. We can summarize the benefit of such a simulation threefold; (1) to optimize satellite design before manufacturing, (2) to optimize satellite transponder utilization for existing satellites and (3) to gain insight of the satellite transponder behavior since a properly developed simulation is like a laboratory implementation of a system where one can make measurements at any point [3].

A simulator to characterize satellite transponder impairments when excited by multicarrier modulated waveforms has been developed based on manufacturing test data of TURKSAT-3A (T3A) satellite, launched in 2008 to provide DTH TV and data transmission services over three continents; Europe, Asia and North Africa. The thesis first introduces satellite transponder structure and describes the communication impairment sources through it. Then the simulation model which consists of transmission, transponder and receiver sections is introduced and the methodology of total degradation assessment is explained. Finally, total degradation results are provided for several transponder utilization scenarios and optimal operating conditions are discussed incorporating obtained results in link budget calculations.

CHAPTER 2

SATELLITE TRANSPONDER STRUCTURE AND SOURCES OF COMMUNICATION IMPAIRMENT

A communication satellite could be categorized either as a bent pipe (transparent) or a regenerative repeater satellite. Transparent satellite systems apply only frequency conversion, amplification and if applicable beam/polarization switching whereas regenerative satellite systems apply on board signal processing, demodulation and multiplexing of incoming signals. Transparent repeaters have widespread use as in the case of TURKSAT satellites all of which are in this configuration. Therefore, this research is conducted upon transparent repeater structure. In this chapter, firstly communication satellite transponder structure is introduced and then communication impairments caused by transponder equipment are explained to establish the basis of simulation model.

2.1. Transponder Structure

A simplified block diagram of a transparent communication satellite payload is provided in Figure 1 and functional explanations are provided below.

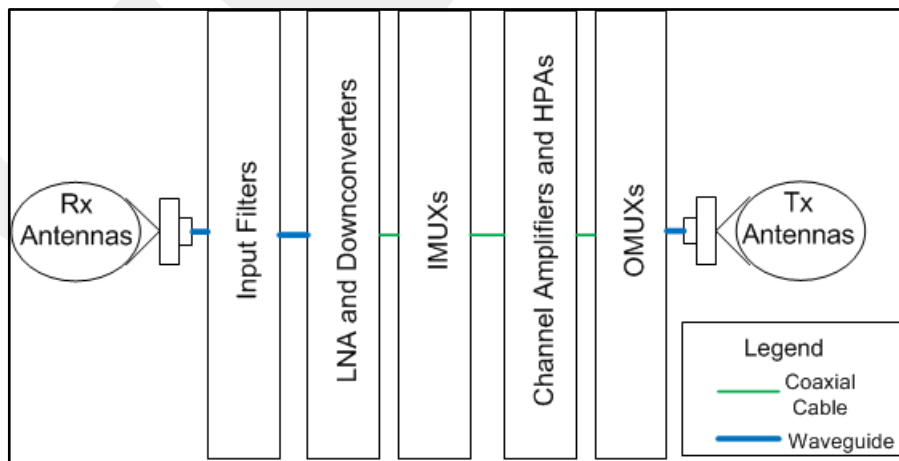


Figure 1 Simplified Transparent Repeater Block Diagram

Receive (Rx) and Transmit (Tx) Antennas: Communication payloads are usually examined in two sections as antenna and repeater subsystems. Antennas are apparently used to receive and transmit electromagnetic (EM) waves. Several types of antennas are used on satellites such as horn, reflector (offset, Cassegrain etc.) and active antennas. Most common antennas used on communication satellites are offset reflector antennas which are deployed on East or West sides of the spacecraft. Current satellites almost always make use of shaped beam antennas which radiate within the service area contours and avoid over-spilling. Satellite operators determine their need of service areas and satellite antennas are designed so as to provide highest gain over this coverage area. In the simulation of transponder performance, we will not model antennas since our focus is only on the transponder bandwidth and antennas are very wideband passive equipment with negligible gain slope in such narrow band. The impact of antennas thus covered in link budget calculations as their contribution to G/T (Gain to noise Temperature ratio) and EIRP (Equivalent Isotropically Radiated Power). G/T is the figure of merit for reception and calculated by the following formula:

$$G/T \text{ (dBK}^{-1}\text{)} = G_{Rx} \text{ (dBi)} - T_S \text{ (dBK)} \quad (1)$$

where G_{Rx} is the receive antenna gain and T_S is the system noise temperature [4]. EIRP is the transmission power capability metric of the satellite and is defined by:

$$EIRP \text{ (dBW)} = P_S \text{ (dBW)} + G_{Tx} \text{ (dBi)} \quad (2)$$

where P_S is the satellite transmit power at antenna feed flange and G_{Tx} is the transmit antenna gain [4].

Input Filter: Input filter is a very wide band waveguide filter receiving the designated satellite operating uplink (U/L) frequency band (like 13.75 – 14.50 GHz in Ku band) and rejecting other Rx and Tx frequency bands. Usually it has very small insertion loss around 0.3dB and negligible impact on channel frequency response and group delay.

Wideband Low Noise Amplifier (LNA) and Down Converters (D/C): LNAs are used for low noise amplification of incoming signals and down converters are used for frequency conversion to downlink band. Usually, LNA and D/C is packaged together and called receiver. A typical Ku band receiver has approximately 2dB noise figure and around 60 dB gain. Another very important performance of the receiver is amplitude linearity measured by C/IM3. A receiver provides around 60 dB C/IM3 ratio inside designated operation input levels. At the design stage, it is assured that the receivers of the satellite will work in this linear region; therefore yet again receivers have negligible performance impairment for a transponder in terms of nonlinearity and intermodulation. On the other hand, local oscillators used in D/Cs will introduce random phase variations, called phase noise which will introduce degradation to the performance of the communication system [5]. Reference [5] provides the results for the impact of phase noise over satellite link where we can see that the degradation caused is around 0.01dB for QPSK and less than 0.1dB for higher modulation types.

Input Multiplexer (IMUX): The input multiplexer is where channelization from wide band to narrow band occurs in repeater. It is composed of power dividers, circulators and channel filters. Usually 27 MHz, 36 MHz or 72 MHz channels are used in communication satellites. In emerging high throughput satellites (HTS), higher transponder bandwidths like 125 MHz are also appearing. An IMUX has several channel band pass filters designated to specific center frequencies.

The signals passing from IMUX filters are considered to be channelized and routed to individual amplifiers. Each channels' filter has to provide enough rejection to adjacent channel frequencies to avoid power robbing at amplification stage (amplification stage is wide band, not specific to channel) and multipath effects. However, sharper the channel filter is, higher the level of group delay at channel edge. The group delay introduced inside channel frequency because of such filter has to be considered in detailed link analysis.

Amplifier Section: Amplifier section consists of Channel Amplifier and High Power Amplifier (HPA).

The channel amplifiers are generally produced with monolithic microwave integrated circuit (MMIC) technology and they have adjustable gain range typically in the order of 20 to 50 dB [6], which is necessary to adjust the power level necessary at the input of the HPA.

The High Power Amplifier is the final amplification stage in the transponder and its output power along with antenna gain determines the EIRP of the satellite. Solid State Power Amplifiers (SSPA) and Travelling Wave Tube Amplifiers (TWTAs) are the two choices for this stage. As explained in [6], SSPAs have become available in early 1980s in C band for space applications and it was predicted that SSPAs would take over from TWTAs thanks to higher linearity and attractive power/mass ratio. In contrary, DC to RF power efficiency and maximum power output properties of TWTAs in Ku and above frequency bands favored them so far. Reference [7] states that, Boeing satellite fleet have utilized 2345 TWTAs and 1076 SSPAs until the year of 2013. Among these, when frequency band distribution is inspected, TWTAs have been used in a wide range of frequencies from S to Ka band whereas SSPAs have been used in lower bands like L, S and C but they were almost never used in Ku and above frequencies. Consistently, T3A satellite has made use of only TWTAs in Ku band.

Current satellites usually incorporate a pre-distortion linearizer as last stage of the Channel Amplifier to compensate for amplitude and phase non-linearities of TWTs. Pre-distortion linearizers are designed to have a circuit with a transfer function opposite to the device to be linearized. Each linearizer has to be tuned perfectly for its TWT mate for better linearization. Such linearizer and TWT pairs are called Linearized TWT (LTWT).

Output Multiplexer (OMUX): Basically OMUX is doing the reciprocal function compared to the IMUXs. All of the channels which are going to be routed to the same antenna port are recombined by the OMUX after amplification stage. However OMUX design is much more stringent since the losses introduced by OMUX are much more critical causing reduction in satellite EIRP. In addition, the amplitude and group delay responses of OMUX filters inside the channel frequency have to be considered in transponder performance analysis just like IMUX.

2.2. Communication Impairments

TWTs and LTWTs, having widespread use in space as high power amplifiers, are nonlinear devices especially when driven near saturation. Nonlinearity causes three harmful effects to the end to end performance; (1) generation of unwanted signals, (2) degradation of overall BER (bit error rate) and (3) EIRP reduction and inefficient use of HPA, necessitating the back-off operation when linearity is concerned [8]. In addition, IMUX and OMUX have in band amplitude and group delay responses those have to be considered in transponder performance characterization.

2.2.1. AM/AM and AM/PM Transfer Curves

In this section, amplitude and phase non-linearities of high power amplifiers are discussed. Figure 2 shows normalized characteristics of a sample TWT as a function of input back-off (IBO) [6]. Figure 2(a) demonstrates P_{in} - P_{out} or AM/AM curve. AM/AM curve relates the input signal power normalized as input back-off (IBO) to output signal power normalized as output back-off (OBO). As displayed, IBO is the difference of operating input power level with respect to the power necessary to saturate the HPA.

$$IBO(dB) = P_{in}(dB) - P_{in,sat}(dB) \quad (3)$$

Likewise, OBO is the difference of operating output power level with respect to saturated HPA output power.

$$OBO(dB) = P_{out}(dB) - P_{out,sat}(dB) \quad (4)$$

The slope of this curve is called AM/AM conversion coefficient and expressed in dB per dB [6]. At sufficiently backed off operating points; the HPA has one to one AM/AM performance but when close to saturation point, non-linearity increases and AM/AM conversion coefficient decreases. This is called gain compression. Gain variation of the TWT is displayed in Figure 2(b). Another result of nonlinear

behavior is the introduction of phase shifts between the input and the output by HPA. Figure 2(c) shows the AM/PM curve of the TWT. This curve relates the input signal power to phase shift. Such non-constant phase shift is especially harmful for digital PSK modulations used in satellite communications since the information is carried by the phase of the signal [8].

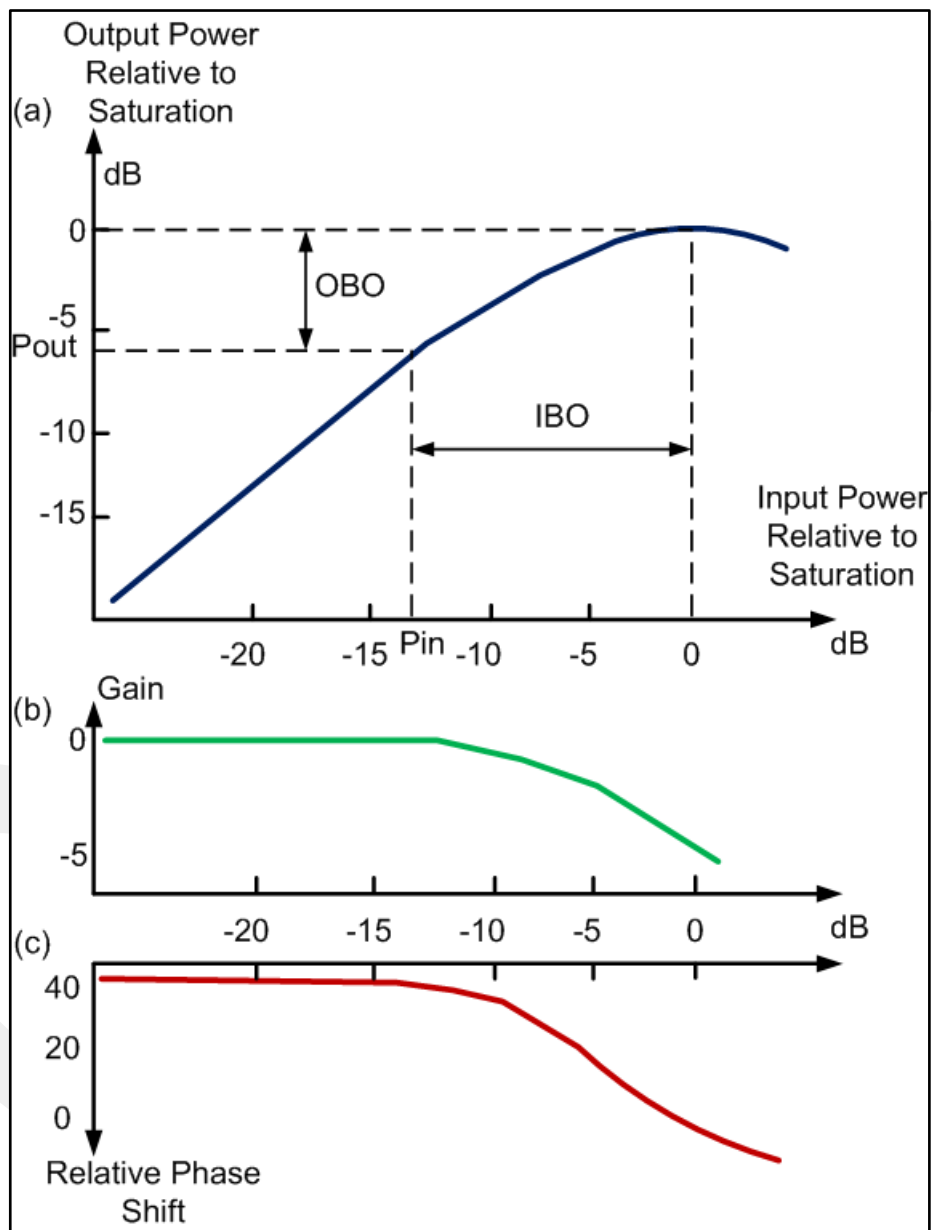


Figure 2 Normalized characteristics of TWT as a function of IBO (a) P_{in} - P_{out} or AM/AM curve (b) Gain Variation (c) Relative Phase Shift or AM/PM curve

Figure 3 shows the AM/AM and AM/PM performances of a T3A TWT and associated LTWT which is used in the simulation.

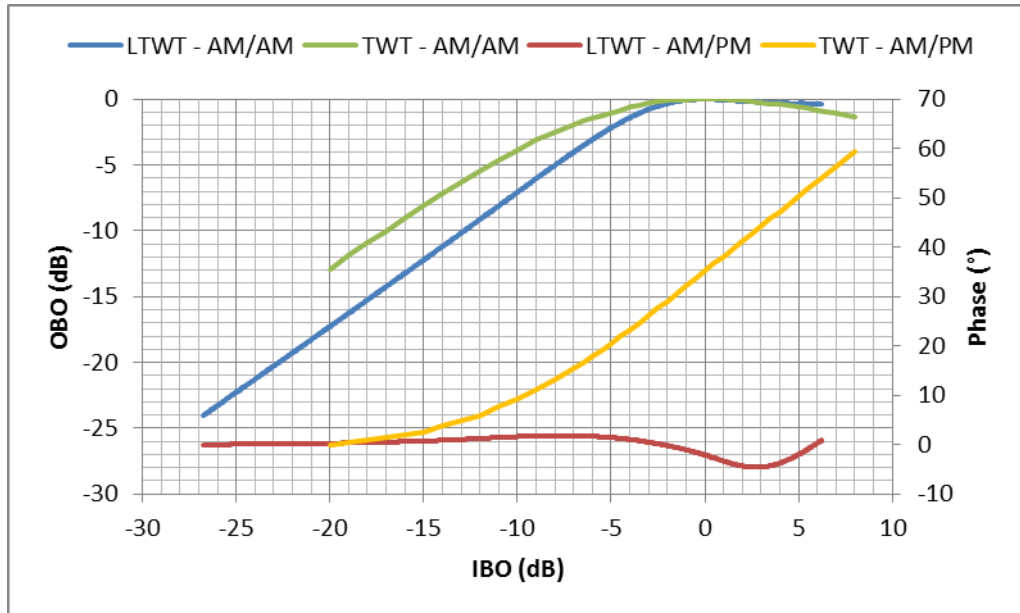


Figure 3 AM/AM and AM/PM responses of a T3A TWT and associated LTWT

Comparing the TWT and LTWT performances, it can be observed that the linear portion of LTWT's AM/AM curve extends towards saturation compared to TWT thanks to the linearizer. Likewise the linearizer dramatically limits the 60° total phase shift over the entire input signal power range to only 7° .

The entire hurdle is about finding the optimum operating point of the HPA over the AM/AM curve which is closest to the saturation point in order not to waste very critical EIRP while not sacrificing the link performance to nonlinear degradations.

2.2.2. Intermodulation (IM)

A nonlinear HPA introduces IM products at integer combinations of input carriers, when multiple carriers are amplified through it. Figure 4 illustrates the power levels associated with two equal amplitude carriers exciting a satellite transponder and the 3rd order intermodulation product levels [6]. In this figure, P_{O1} represents single

carrier operation output power and P_{O2} represents two carrier operation output power for one of the carriers. Comparing these two curves, the maximum power in single carrier operation is higher than that of two carrier operation. So, the maximum power is shared among the two input carriers and intermodulation products.

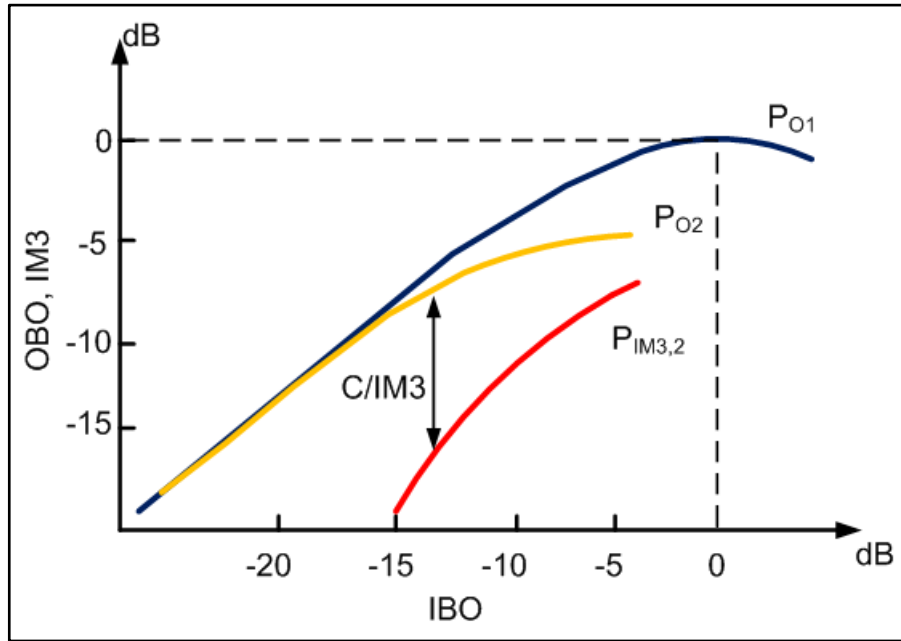


Figure 4 Normalized power transfer characteristics with two unmodulated carriers

$P_{IM3,2}$ represents 3rd order intermodulation product power level for one of the 3rd order products. The difference between actual carrier's output power (P_{O2}) and 3rd order intermodulation product power is defined as carrier to third order intermodulation noise ratio; $C/IM3$.

$$C/IM3 (dB) = P_{O2}(dB) - P_{IM3}(dB) \quad (5)$$

Since the intermodulation power is increasing towards saturation, $C/IM3$ decreases in non-linear operation region which is not desirable for overall link performance. The IM power decreases with the order. In satellite communications, since the operating bandwidth is much smaller than the operating frequency, i.e. at least two orders of

magnitude smaller, even-order products fall out of band and only odd-order products, especially third order (IM3), are of concern [8].

There are many strategies proposed in the literature for IM reduction or avoidance by means of frequency plan assignment as in [9], however these methods have some drawbacks, the most prohibitive one being the waste of invaluable satellite spectrum resources. Therefore, frequency plan assignment strategies have to be considered as guidelines in satellite operation as a tool to mitigate IM degradation if circumstances such as the available spectrum and carrier configuration allow so.

The well-known IM mitigation method is to drive the satellite HPA into linear region trading EIRP for linearity and causing inefficient use of payload resources. Earlier satellites with highly non-linear TWTs had to be operated at extremely high OBO levels such as 6-7 dB which means 80% of the available TWT power is not used to mitigate the IM distortion. However advances in pre-distortion type linearizers which are well suited for satellite communication frequency range and bandwidth needs, aid satellite operators to drive the satellite HPAs further close to saturation region without suffering from IM distortion. References [10, 11] cover the pre-distortion linearization technique in great detail and discuss the benefits depending on the frequency band, total bandwidth and operation back-off levels. A very brief conclusion to be reported from both is that the linearizers provide at least 10 dB increase in IM, harmonic and NPR performances for space TWTs. No wonder they are broadly used in recent satellites as in the case of T3A under study. Figure 5 shows the measured C/IM3 performance of a T3A TWT and its linearized version, LTWT. The given IBO levels are for one of the two unmodulated carriers used in the test with respect to single carrier saturation power. The improvement provided by the linearizer is easily noticed. There is also an intentional first peak around -9 dB IBO for one carrier, corresponding to -6 dB IBO for total input power. A peak around this IBO level is quite useful in order not to waste too much output power for linearity.

As explained above C/IM3 performance is measured during manufacturing of satellites and used in link budget calculations to take IM distortion into account. However, since it is measured with two unmodulated carriers, this data alone is not representative of multiple modulated carriers.

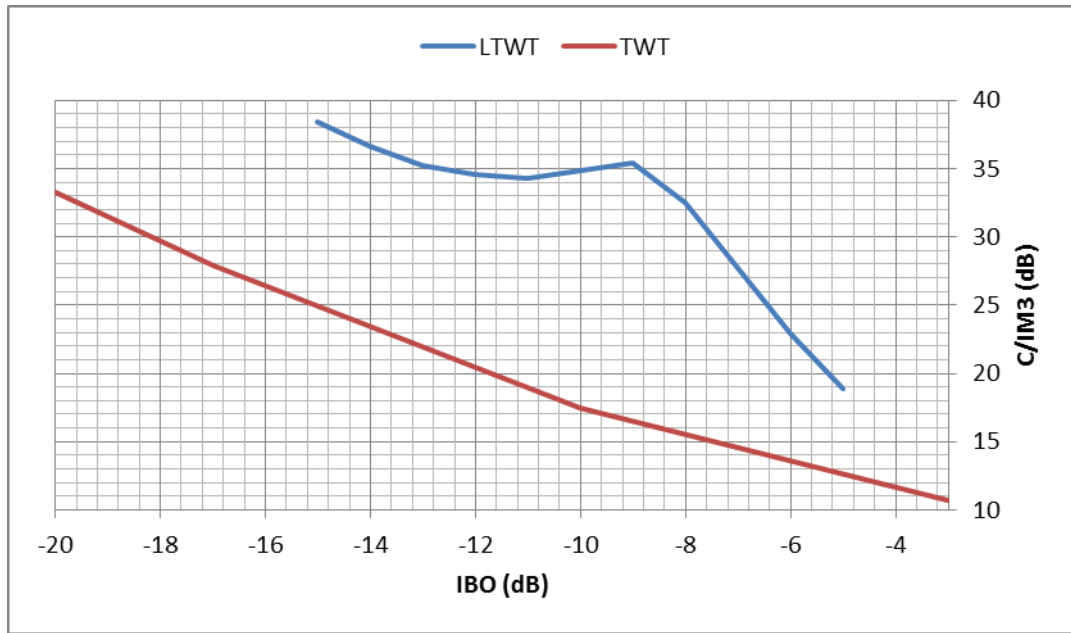


Figure 5 C/IM3 performance of a T3A TWT and associated LTWT

2.2.3. Noise Power Ratio (NPR)

While C/IM3 is measured with two CW (continuous wave) carriers, there is another linearity metric called Noise Power Ratio (NPR) characterizing the performance of HPA when it is excited by infinite number of carriers [6]. NPR measurement consists of feeding the HPA under test with notch filtered random white noise and comparing the power spectral densities (PSD) outside and inside of the notch by the following formula:

$$NPR (dB) = 10 \log(N_0/N_{0,IM}) \quad (6)$$

where N_0 is the noise PSD outside of the notch and $N_{0,IM}$ is the noise PSD inside the notch as shown in Figure 6 below.

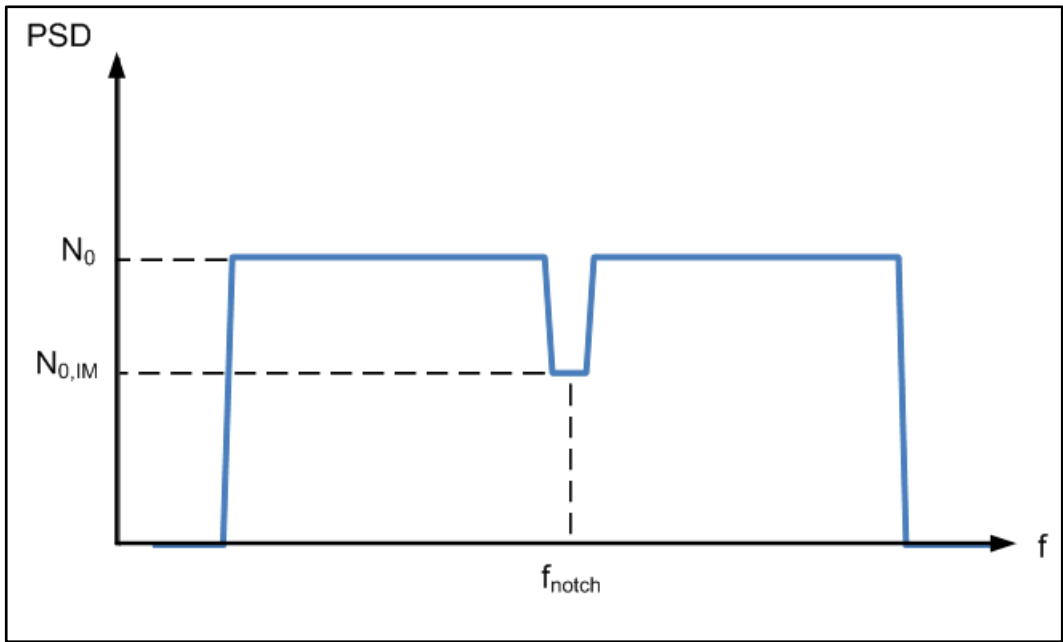


Figure 6 NPR Measurement

Figure 7 shows NPR performance of the same LTWT for which the C/IM3 performance provided previously.

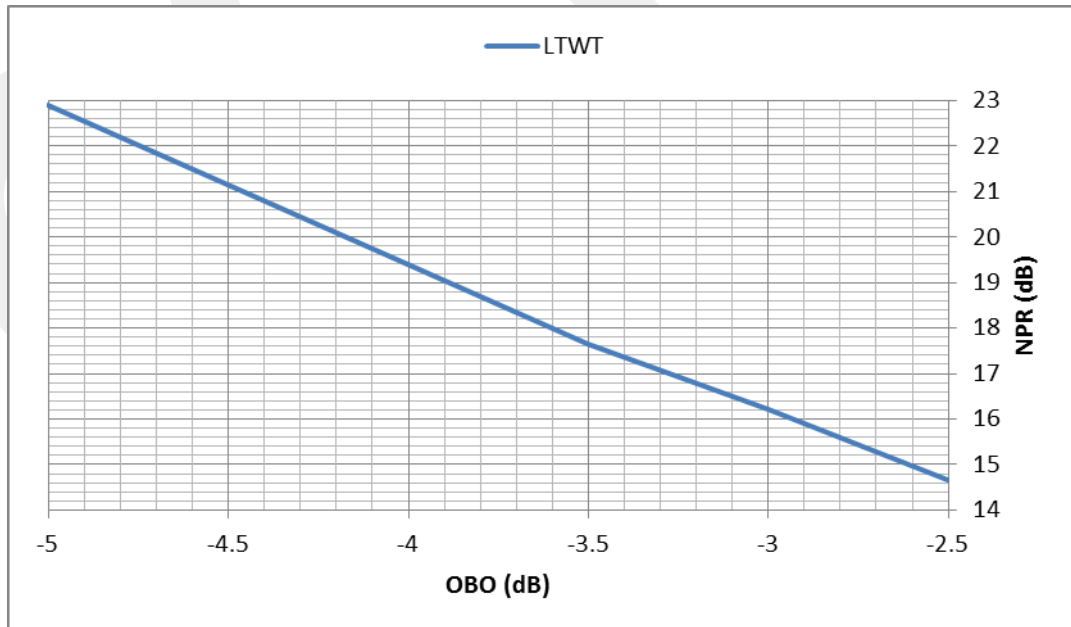


Figure 7 NPR performance of a T3A LTWT

Please note that this figure reflects the performance with respect to OBO. To compare with previous figure, it is necessary to subtract 5dB from OBO. For instance, at -2.5dB OBO Figure 7 represents 14.5dB NPR performance, which corresponds to the 30dB C/IM3 performance at -7.5dB IBO given in Figure 5. There is roughly 15dB C/I difference at this operation point. Comparing C/IM3 with NPR, C/IM3 is measured with two CW tones whereas NPR represents the performance for infinite number of carriers. Therefore, as discussed in [12], given an actual satellite HPA operating scenario with modulated carriers, C/IM3 is optimistic while NPR is pessimistic in many cases. We have explored that there is a considerable 15 dB difference for a given operation point between these two metrics in our case. Thus, this is another area where transponder simulations help us to solve the riddle of exact degradation level.

2.2.4. Filters' Amplitude and Group Delay Responses

Figure 8 shows the amplitude and group delay responses of a T3A OMUX channel. Both IMUX and OMUX have similar responses that have to be considered in transponder performance analysis. This is a 36 MHz channel and the performance show sharp rejection after 20 MHz distance from channel center to reject any unwanted emissions to adjacent channels.

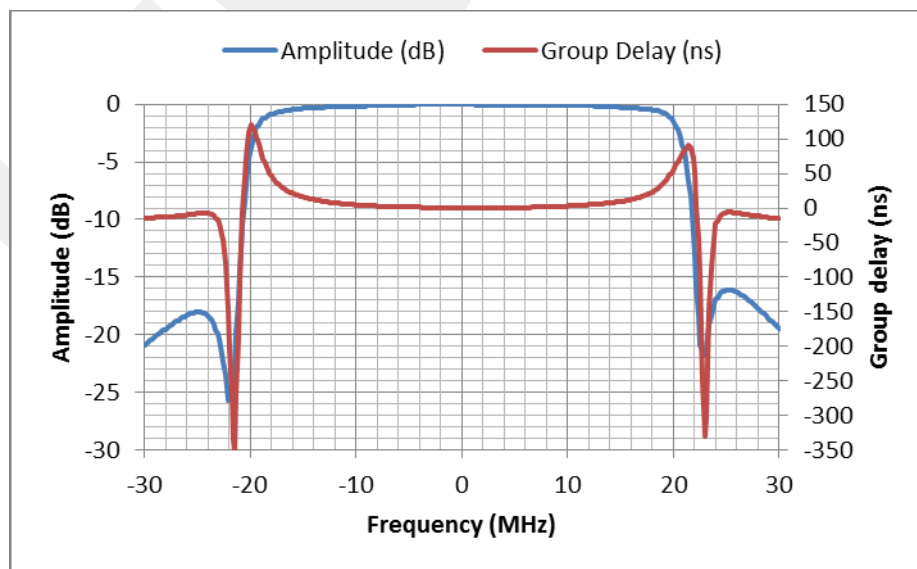


Figure 8 Amplitude and Group Delay responses of a T3A OMUX Channel

A sharp amplitude rejection just next to pass-band of a channel is necessary to narrow the guard band between channels. Cost of a sharp rejection, in contrast, is facing with a high level of group delay variation especially towards the channel band edge as visible in Figure 8. Group delay is the derivative of filter phase transfer function with respect to frequency [5] and it causes distortion of different frequency components with varying delays through filter, which in turn results in unwanted quadrature components causing crosstalk [13]. Therefore, ISI will arise for carriers operated at channel edge.

CHAPTER 3

SIMULATION SYSTEM MODEL

Satellite communications, first introduced in late 1950s have been widespread dramatically and proven to be an integral part of today's wireless world. The cost and non-touchable characteristics when launched make communication satellite design very critical. Earth segment prices are also considerable and complete link should be optimized before deployment as accurate as possible to mitigate any risk. Recent advances in communication systems are driving the complexity of these systems to higher levels where it is almost impossible to design and analyze them without software aid. Thus, developing a simulator would help satellite communication experts in design of satellite payload and communication networks by providing detailed insights to non-linearities inherent in satellite transponders which are not captured by ordinary link budget tools.

A satellite transponder simulator is necessary for below reasons:

- to optimize satellite design before manufacturing
- to identify the root cause of link problems
- to be able to test the impact of any changes either on ground or on orbit before implementation
- to optimize satellite transponder utilization and link performances
- to gain insight of the satellite transponder behavior.

In the field of satellite communication link modeling and analysis, the regular approach is using a link budget calculator in order to make an assessment on whether a link can be closed (i.e. the receiver's threshold E_b/N_0 level can be reached) or not. Such link budget calculations take into account all gains and losses introduced in the satellite link as well as noise contributors and atmospheric losses such as rain attenuation faced at high frequencies used in satellite communications. When all necessary inputs are supplied to link budget calculators, it is possible to get necessary uplink power requirements and resulting overall C/N and E_b/N_0 values.

Although link budget calculators constitute an easy and fast way to determine a satellite link's performance, it has limited assessment on the impairments caused by filtering and HPA non-linearities. DVB standards, for instance, provides threshold E_s/N_0 figures for AWGN channel without any degradation caused by real transponder equipment and it mentions that "for calculating link budgets, specific satellite channel impairments should be taken into account" [1]. To fill in this gap, a simulator to characterize satellite transponder impairments when excited by multicarrier modulated waveforms has been developed based on manufacturing test data of T3A satellite through this thesis study. This chapter examines the simulation system structure in three sections; transponder model, transmission model and receiver model.

3.1. Transponder Model

The satellite transponder is modeled as depicted in Figure 9. Using IMUX/OMUX filters and high power amplifier to model a transponder is quite realistic since other filters like input filter or active equipment are very wideband and have negligible impact over transponder performance as discussed previously. The same approach has been followed in many other studies [12, 14, 15 and 16]. As mentioned previously, a distinctive aspect of this simulation is to be built upon real test data of a T3A transponder to focus on actual performance. The modeled transponder is a 36 MHz Ku band transponder which can be utilized for both DTH TV and data transmissions.

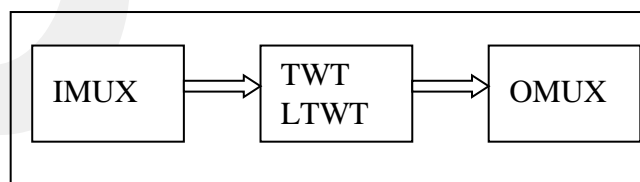


Figure 9 Simulation Transponder Model

IMUX and OMUX Filters: Instead of using built in standard filters, IMUX and OMUX filters are modeled by using their amplitude response and group delay response curves to construct filters' impulse responses.

In order to construct the FIR (Finite Impulse Response) filter impulse responses of T3A IMUX and OMUX filters from the measured data, the methodology defined in [3] is followed, as briefly summarized in below steps:

1. The bandpass frequency response data is converted to lowpass data by simply relabeling the frequency axis as $f_{\text{lowpass}} = f - f_c$.
2. The available data is resampled with N , where N is the number of samples of the impulse response. Linear interpolation is used among the available test data for this process.
3. Group delay data is converted to phase response by numerical integration over frequency.
4. Frequency response data is extended to $-f_s/2$ to $f_s/2$. Sampled transfer function $H(f)$, $-f_s/2 < f < f_s/2$ is obtained where
 - $f = k \Delta_f$
 - $k = -N/2$ to $N/2-1$
 - $\Delta_f = 1 / (NT_s)$ (frequency resolution)
 - f_s : sampling rate, $T_s = 1 / f_s$ (sampling time)
5. Negative frequency portion of the $H(f)$ is moved to $N/2+1$ to N . Now $H(k \Delta_f)$ where $k=1, 2, \dots, N$ contains frequency response.
6. Inverse FFT is taken to acquire the impulse response.

The magnitude and group delay responses of a T3A OMUX filter constructed in simulation by this method are presented in Figure 10 and Figure 11 respectively, in comparison with the measured data. By inspecting these magnitude and phase responses of the simulated filters for IMUX and OMUX, the validity of the simulated filters are verified.

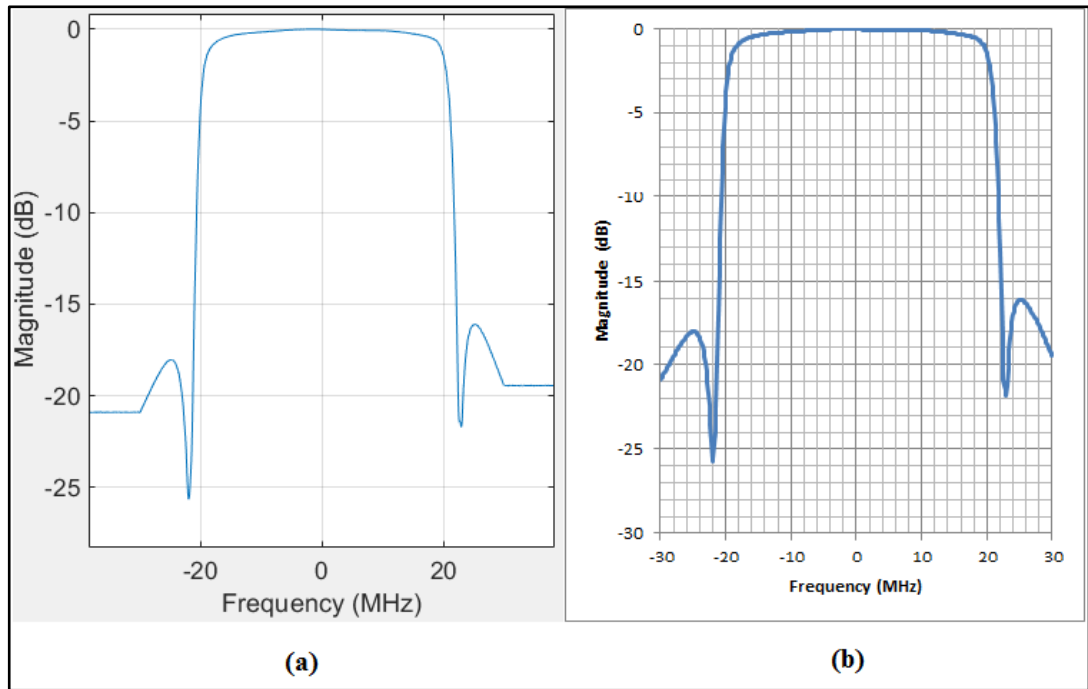


Figure 10 T3A OMUX filter (a) constructed magnitude response (b) measured magnitude response

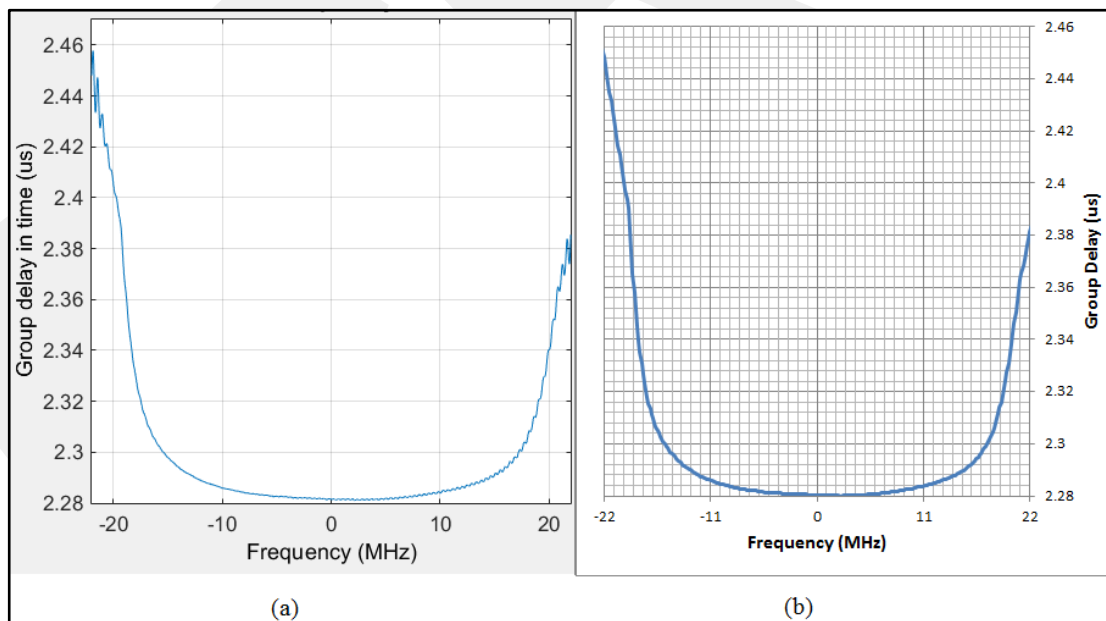


Figure 11 T3A OMUX filter (a) constructed group delay response (b) measured group delay response

TWT and LTWT: In the literature, there are many studies on nonlinear modeling of TWT amplifiers. Saleh, being one of the most famous in this area, presented simple

two parameter formulas to represent AM/AM and AM/PM functions of a TWT as given below [3, 17]:

$$f(A) = \alpha_f A / (1 + \beta_f A^2) \quad (7)$$

$$g(A) = \alpha_g A^2 / (1 + \beta_g A^2) \quad (8)$$

where $f(A)$ and $g(A)$ are AM/AM and AM/PM responses respectively; A is input signal power; α_f , α_g , β_f and β_g are modeling parameters. Experimental data is approximated by adjusting modeling parameters of these equations using curve fitting techniques. Then the obtained equations are used in analytical derivations of the TWT behavior.

In the simulation, a similar approach is followed. TWT and LTWT are modeled by their respective AM/AM and AM/PM curves as memoryless nonlinearity with unity gain. Instead of approximation by such functions though, numerical interpolation of the experimental data is performed. Memoryless nonlinearity applies here since the bandwidth of the TWT is much higher than the transponder bandwidth, i.e. 1.8 GHz versus 36 MHz in Ku band and there is negligible group delay variation in transponder bandwidth introduced by the TWT.

Below are the steps followed in TWT and LTWT modeling which is performed in time domain as complex envelope model [3]:

1. The average power of the input signal is normalized to the specified IBO level
2. The input amplitude and phase are calculated from the samples of complex envelope of the input signal
3. Output amplitude is calculated from AM/AM data using interpolation
4. Output phase offset is calculated from AM/PM data using interpolation
5. Complex envelope representation of the output signal is constructed by the following formula:

$$\tilde{z}(t) = f(A(t)) \exp(jg(A)) \exp(j\phi(t)) \quad (9)$$

where $A(t)$ is input signal, $f(A(t))$ is output amplitude, $g(A)$ is output phase offset and $\phi(t)$ is input phase. IBO level is the only input parameter to the TWT model.

3.2. Transmission Model

3.2.1. Carriers

Over the 36 MHz bandwidth of the transponder, scenarios of a single full band carrier, dual carriers and 8 narrow band carriers are considered to represent actual transponder utilization as listed in Table 1 and shown in Figure 12. When there are two or more carriers they are combined by FDM (Frequency Division Multiplexing). In order to limit the number of scenarios and associated results to be presented to a reasonable amount, comparison of multicarrier cases are modeled in QPSK only whereas higher modulation schemes are compared in single carrier scenario.

Table 1 Simulated Carrier Scenarios

<i>N</i> <i>o</i>	<i>Carriers</i>	<i>Symbol Rate</i> <i>(Ksps)</i>	<i>Roll</i> <i>-</i> <i>off</i>	<i>Bandwidth</i> <i>(MHz)</i>	<i>Guard</i> <i>Band</i> <i>(MHz)</i>
1	Single QPSK Carrier	30000 (33, 36, 38 Msps) ^a	20%	36	-
2	Two QPSK Carriers	14800	20%	2 x 17.76	0.24
3	Eight QPSK Carriers	3500	20%	8 x 4.2	0.3 ^b
4	Single 8PSK, 16APSK, 32APSK, 64APSK and 256APSK carrier	30000	20%	36	-

^a. Listed increasing symbol rates are also analyzed comparatively

^b. Lower guard bands are as well analyzed versus ACI

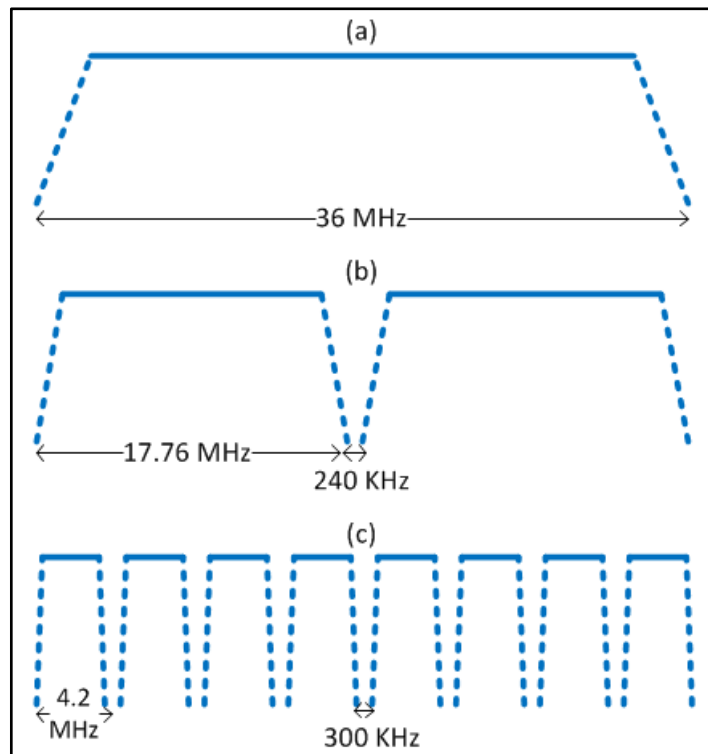


Figure 12 Simulated Carrier Placements over the 36 MHz Transponder

3.2.2. Modulations

Several modulations from DVB-S, S2 and S2X [1, 2, 18] are manually implemented in the simulation by constructing their respective constellations. Random symbol sequences are generated and mapped into the selected constellation.

QPSK and 8PSK are utilized in both DVB-S and DVB-S2 and they are still the most widely used satellite communication waveforms providing the lowest E_b/N_0 threshold levels necessary for DTH TV transmissions. These modulations are also utilized for return data links (remote terminal to gateway station) of satellite data networks.

16APSK and 32APSK modulations have been introduced in DVB-S2 and implemented in simulation as defined there. These modulations are aiming higher data rate per bandwidth (bps/Hz) efficiency when the satellite link can tolerate higher thresholds and they are used in data links as forward link (gateway station to remote terminal) modulation type. DVB-S2X introduces different implementations in terms

of constellation mapping for these modulations. 16PSK and above PSK modulations are not defined in DVB standards since APSK modulations are more efficient i.e. require less E_s/N_0 for the same level of BER. In the simulation, these are implemented just for comparison reasons.

In addition, 64APSK and 256APSK modulations which are recently introduced in DVB-S2X are implemented in the simulation. Just like 16 and 32APSK modulations these are aiming much higher link efficiencies. However, their threshold E_s/N_0 levels are around 14-20dB range for AWGN linear channel [2] and they are much prone to transponder and earth station equipment impairments, thus they may find quite rare usage in practice.

The constellation diagrams of aforementioned modulations simulated in AWGN linear channel environment are presented in Figure 13, Figure 14 and Figure 15. These constellations are taken with a block of 50000 symbols and with varying E_b/N_0 levels given over the figures. Red stars at the center of each cluster show the ideal symbol locations.

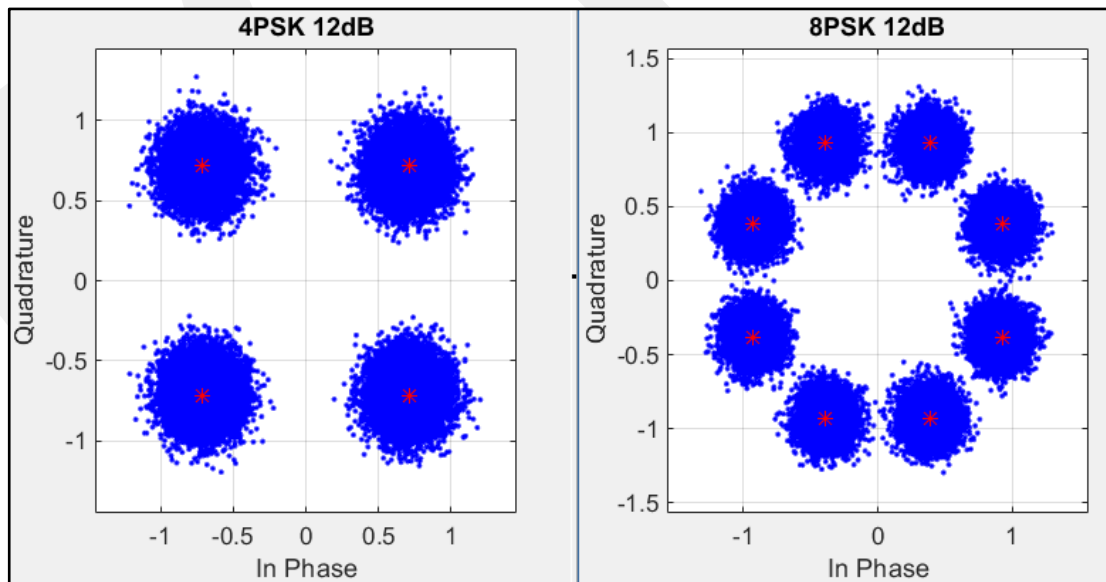


Figure 13 QPSK and 8PSK modulations, AWGN linear channel

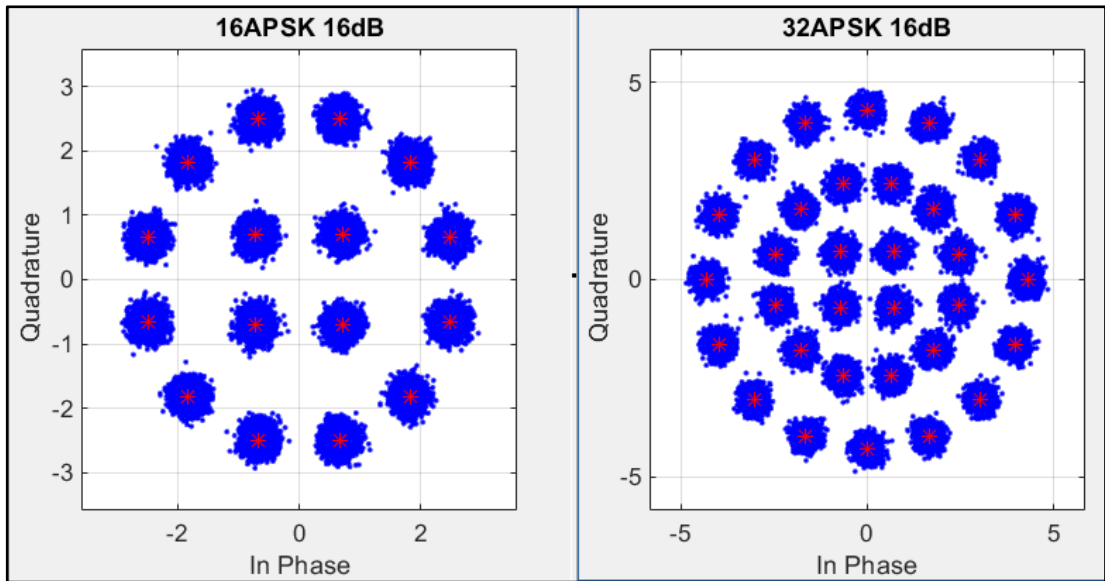


Figure 14 16APSK and 32APSK modulations, AWGN linear channel

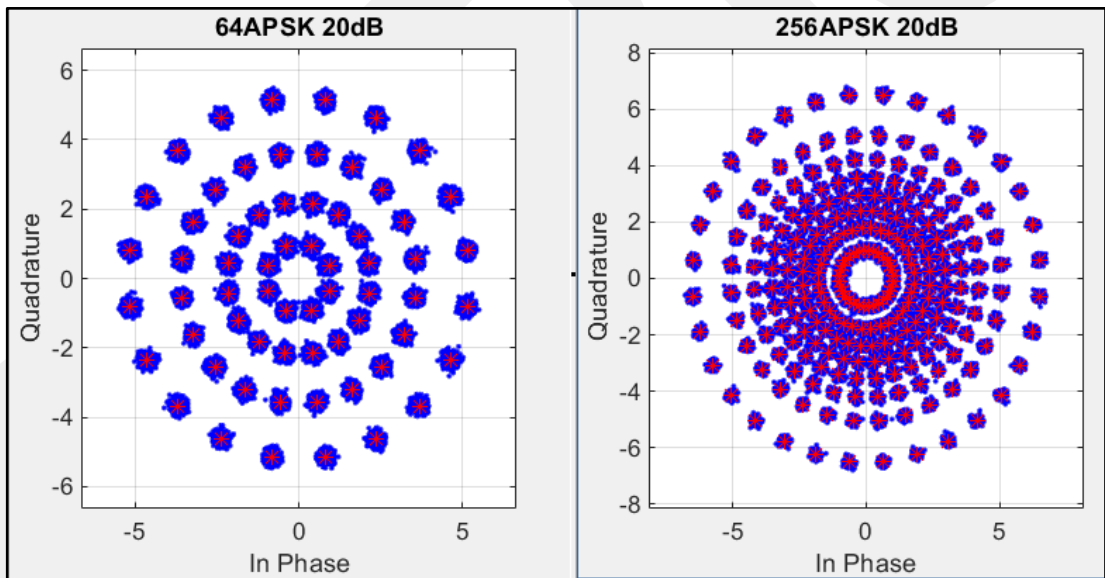


Figure 15 64APSK and 256APSK modulations, AWGN linear channel

3.2.3. Transmit Filter

As necessitated by the DVB standard [1], square root raised cosine (SQRC) filter is used for baseband shaping of the uplink signals. The impulse response of the filter is given by the following equation [3],

$$h_r(t) = (8\beta) \frac{\cos[(R + 2\beta)\pi t] + (8\beta t)^{-1} \sin[(R + 2\beta)\pi t]}{(\pi\sqrt{R})[1 - (8\beta t)^2]} \quad (10)$$

where β is roll-off factor and R is symbol rate. The impulse response is plotted in Figure 14.

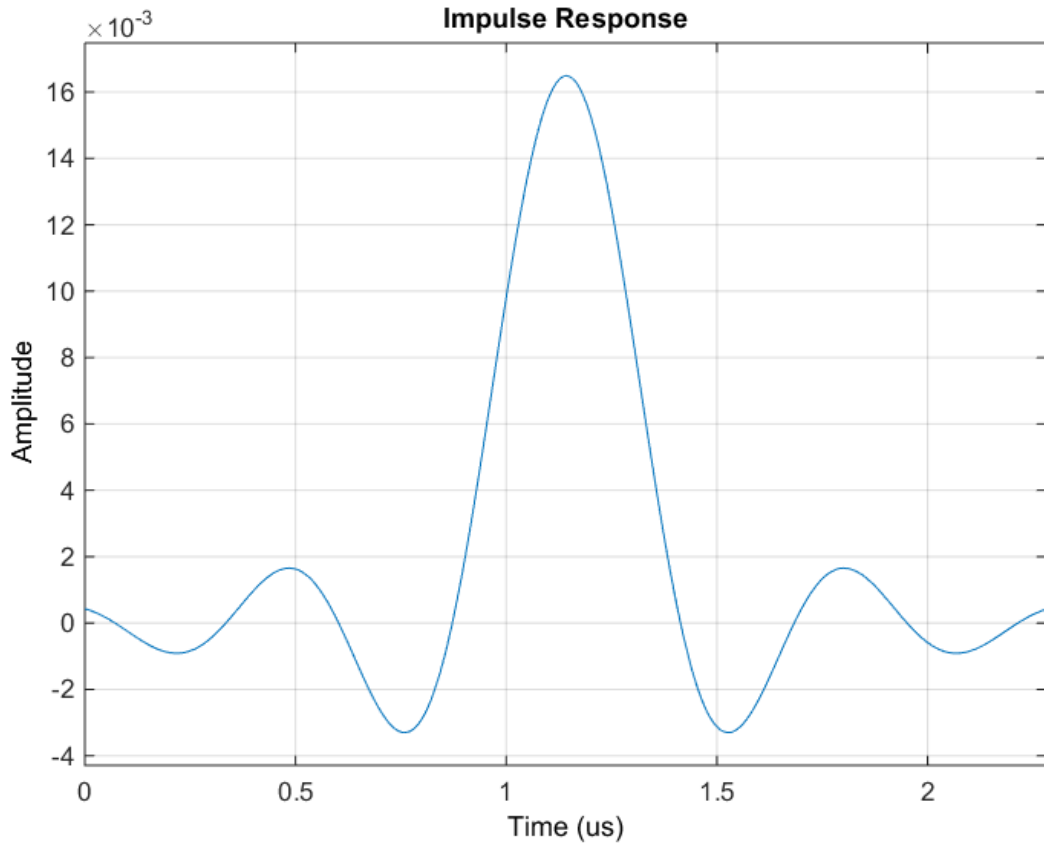


Figure 16 Impulse Response of Transmit SQRC Filter

3.2.4. Uplink Signal Simulation

As explained above there are single, dual or 8 carrier scenarios. Different phase offsets and time delays are introduced for any of these carriers to represent random propagation delays from different uplink stations to the satellite as formulized below [3];

1. The k^{th} carrier is defined by:

$$s_k[n] = \sum_{m=1}^N (A_{km} + jB_{km}) \delta\left(\frac{n}{f_s} - kT_s - \tau_k\right) \quad (11)$$

where;

- A_{km} and B_{km} are direct and quadrature components of the input signal,
- $k = 1, 1 \leq k \leq 2, 1 \leq k \leq 8$ for single, dual and multicarrier scenarios respectively
- f_s is the sampling frequency
- T_s is the symbol time
- τ_k is time delay
- N is the total number of symbols

2. The k^{th} filtered carrier is defined by convolution of carrier with transmit filter's impulse response:

$$x_k[n] = s_k[n] \otimes p[n] \quad (12)$$

where $p[n]$ is impulse response of the transmit filter.

3. The k^{th} modulated carrier is defined by:

$$y_k[n] = a_k \otimes x_k[n] \otimes \exp\left[j\left(\frac{2\pi n f_k}{f_s} + \theta_k\right)\right] \quad (13)$$

where;

- a_k is the amplitude of the k^{th} carrier which is specified by the user
- f_k is the frequency of the k^{th} carrier and adjusted depending on the number of carriers and transponder bandwidth
- θ_k is the phase offset.

4. The combined FDM signal is given by the summation of each carrier:

$$z[n] = \sum_{k=1}^K y_k[n] \quad (14)$$

3.3. Receiver Model

Complementary operations to the transmit side are performed to implement the receiver model in the simulation. The operations performed are summarized below:

- AWGN samples are introduced to the transponder output depending on the user defined E_b/N_0 level.
- The input and output signals are cross correlated. Time and phase offsets are determined. Input signal is adjusted for comparison by determined time and phase offsets.
- The output carrier is multiplied by $\exp(-j2\pi f_i k T_s)$ where f_i is the frequency of the carrier we would like to demodulate and measure.
- Demodulated carrier is SQRC filtered.
- Semianalytic (SA or Quasianalytic) BER analysis is used to characterize QPSK modulations whereas Monte Carlo (MC) BER analysis is used for all waveforms.
- The final output of the system is Symbol Error Rate (SER) which is then converted to BER. E_b/N_0 vs. BER curves are plotted to characterize the degradation caused by the transponder.
- It is also possible to get spectrum or constellation plots at any point in the simulation path. Power spectrum plots taken at various points of the transmission path are supplied in Appendix B for single, dual and 8 carrier scenarios.

Regarding the BER analysis used in the simulation, two different approaches are practiced as mentioned above. If we compare SA BER analysis with MC, the MC BER estimation is applicable to any communication system and it consists of running extensive random experiments on the system until the BER performance is confidently characterized [19]. No analytical knowledge of the system is required for MC BER estimation but the drawback is the long run times required to execute the

simulation [3]. SA BER estimation is on the other hand very fast and drives BER results for a range of E_b/N_0 instead of just one E_b/N_0 value. However, it requires analytical derivation. Given these natures of BER estimation methods, SA method is applied for QPSK modulation and with very fast results available many different carrier scenarios are evaluated with this modulation. The SER of QPSK modulation with SA technique is given by below equation [3];

$$P_s = \frac{1}{N} \sum_{k=1}^N \left\{ Q \left(\frac{Re \{ \tilde{S}_k \}}{\sigma_n} \right) + Q \left(\frac{Im \{ \tilde{S}_k \}}{\sigma_n} \right) \right\} \quad (15)$$

where \tilde{S}_k is k^{th} transmitted symbol in a total of N symbols and σ_n is noise variance.

MC BER estimation, is alternatively used to characterize higher level modulations. SA technique can produce results with just 1000 symbols whereas with MC method millions of symbols have to be processed depending on the error rate. Therefore block serial approach is applied in order not to run out of computer RAM. In block serial approach, blocks of 50K symbols processed at a time and filter states recorded, then the new block processed with filter state from previous run. AWGN is added to the output symbol sequence depending on the E_b/N_0 level defined as an input to the simulation. Before comparing input and output constellations, the ideal locations of transmit signal constellation is adjusted so that both constellations have the same average power, otherwise they cannot be compared. The symbol decision is performed with maximum likelihood criterion. The output symbol's distance to ideal constellation points are calculated and the symbol is decided to be in the symbol group with minimum distance.

Various sanity checks have been performed on the simulation results including comparison of SA, MC and theoretical BER levels. An example is given in Figure 17 for QPSK signal.

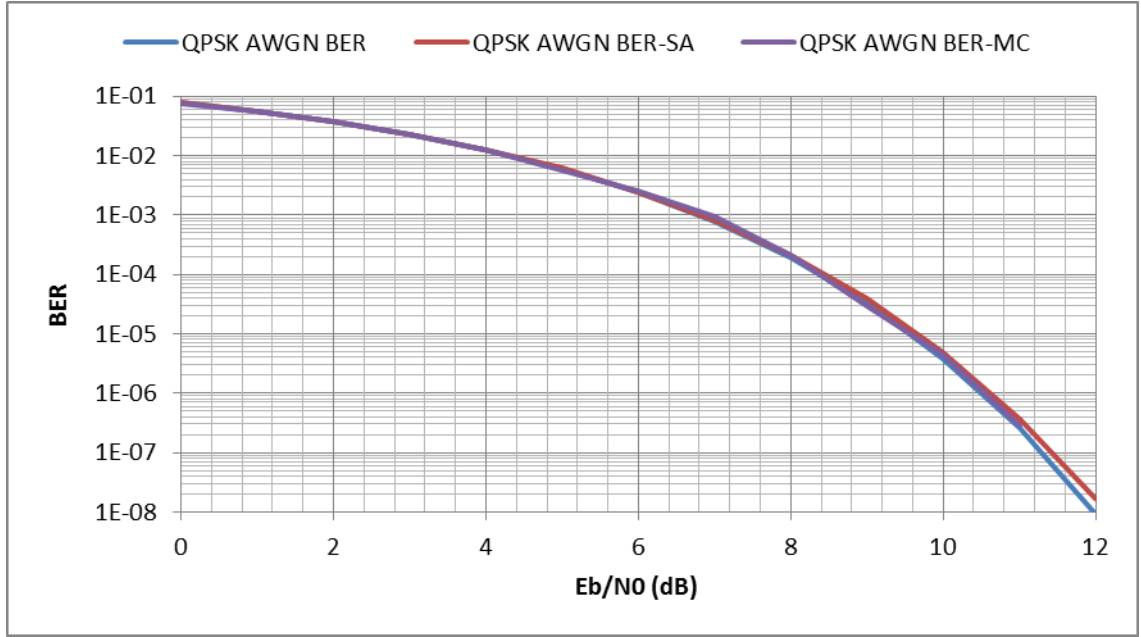


Figure 17 Comparison of Theoretical BER with SA and MC Simulated BER

The error probability of QPSK signal through AWGN channel is given by below equation [20]:

$$P_b = Q\left(\sqrt{\frac{2E_b}{N_0}}\right) \quad (16)$$

The other two curves are obtained with the simulation by SA and MC BER estimation techniques. To estimate AWGN BER with simulation the Tx and Rx filters and the transponder is short circuited or in other words these sections are bypassed. This also provides a method to obtain AWGN BER curves for APSK modulation schemes which is very beneficial since analytic formulations are not available for them.

The overlap of all three curves shows us the validity of both modulation and MC/SA BER analysis implementations. It has to be noted that characterization of very low level BERs is very time consuming with MC technique since around 100 times the 1/BER bits has to be simulated through the system. For instance when BER equals to 10^{-6} , around 10^8 bits have to be processed to have a confident BER analysis. Conveniently it is not necessary for our case to characterize such low BER levels since we are aiming to model uncoded data stream and concentration will be at $2 \cdot 10^{-4}$ BER as it will be explained later.

CHAPTER 4

TOTAL DEGRADATION ANALYSIS

Once the simulation has been set up properly, the attention is turned on the problem of how to quantize the impairments caused by satellite transponder which is usable in link budget calculations to obtain optimal operating points. The researchers dealing with this question put forth different approaches and defined TD figures to compare the scenarios under study with ideal case as we are going to examine briefly.

A conventional method to characterize the degradation is to obtain BER vs. E_b/N_0 curves and to calculate the increase in required E_b/N_0 for a specific BER value comparing the transponder response with ideal case. Reference [16] follows this approach and defines TD as:

$$TD(dB) = IBO(dB) + \Delta(dB) \quad (17)$$

$$\Delta(dB) = SNR_{HPA}(dB) - SNR_{Linear}(dB) \quad (18)$$

where Δ is the increase in threshold SNR, SNR_{HPA} is threshold obtained with non-linear TWT and SNR_{Linear} is the threshold in ideal case. The TD defined in equation (17) considers IBO parameter which has to be related with OBO in order to be used in link budget calculations directly.

PER (packet error rate) vs. E_s/N_0 curves are used in [5] to characterize the degradation similarly i.e. the rise in required E_s/N_0 . This study provides the degradation figures individually for different contributors such as AM/AM and group delay, and then suggests combining them by root sum square (RSS). Finally, TD obtained in this approach is offered to be added to the linear E_s/N_0 requirements in link budget calculations. A specific operating point in terms of OBO is pre-determined as constant in this study.

In a comprehensive study to define the linearity requirements of space TWTs, TD is given by the following formula:

$$TD_{dB}^{RF} = OBO_{dB}^{mod} + D_{dB} \quad (19)$$

where the modulated OBO (OBO_{dB}^{mod}) is the loss in EIRP caused by using non-constant envelope signals compared to CW single carrier operation [12]. D is called the demodulation loss and is calculated just the same as Δ explained previously. Reference [12] also proposes a method to measure the TD in simulation environment by means of a notch filter just like the usual NPR test method, assuming the overall signal impairments can be modeled with additive Gaussian random variable uniformly distributed over the signal bandwidth. Obtained parameter is called NPR_n , where n being the number of modulated carriers excited to the TWT. This is certainly an accurate way of determining IM degradations for multicarrier modulated scenarios instead of depending only on C/IM3 or NPR results. The drawback of this method could be asserted as the modification of input signal although it has negligible impact on the result. It should be noted that this method focuses on IM characterization only and hence cannot be used to characterize overall degradation. Another method to characterize the TWT nonlinearity is cross correlation of the TWT output signal with the input signal in order to distinguish the useful power at TWT output from the interfering power [15]. To make an accurate assessment of the IM distortions, this method is superior to the previously explained notch method since there is not any modification on the input signal. However, this method again characterizes only IM distortions.

Among several approaches, one has to apply the most appropriate way of quantifying the impairments based on the specifications of the study. In our case, since TD caused by all impairments is to be determined, the analysis based on BER vs E_b/N_0 curves suits best. Below definition will be adopted in TD calculations:

$$TD(dB) = OBO_{mod}(dB) + \Delta(dB) \quad (20)$$

$$\Delta(dB) = E_b/N_0^{system} (dB) - E_b/N_0^{ideal} (dB) \quad (21)$$

where Δ is E_b/N_0 threshold increase caused by the system compared to ideal case and OBO_{mod} is the loss in output power caused by operation at back-off and modulation

loss compared to CW saturation. This is a combination of methods discussed previously. Here TD is related with OBO in the case of modulated carriers and degradation caused by the transponder which is measured as E_b/N_0 threshold increase. This approach is chosen for the reason that it completely characterizes the degradation occurring through the transponder which can directly be incorporated in link budget calculations.

Figure 18 shows the results obtained for an IBO of -3dB with single QPSK carrier. Figure 18 (a), (b) and (c) parts show spectrum, constellation and E_b/N_0 vs BER curves of the received signal respectively. Figure 18 (c) also displays the assessment of Δ calculated for a BER of 2×10^{-4} which is asserted as a quasi-error free BER level after coding [18]. This is the method used to determine Δ throughout the thesis.

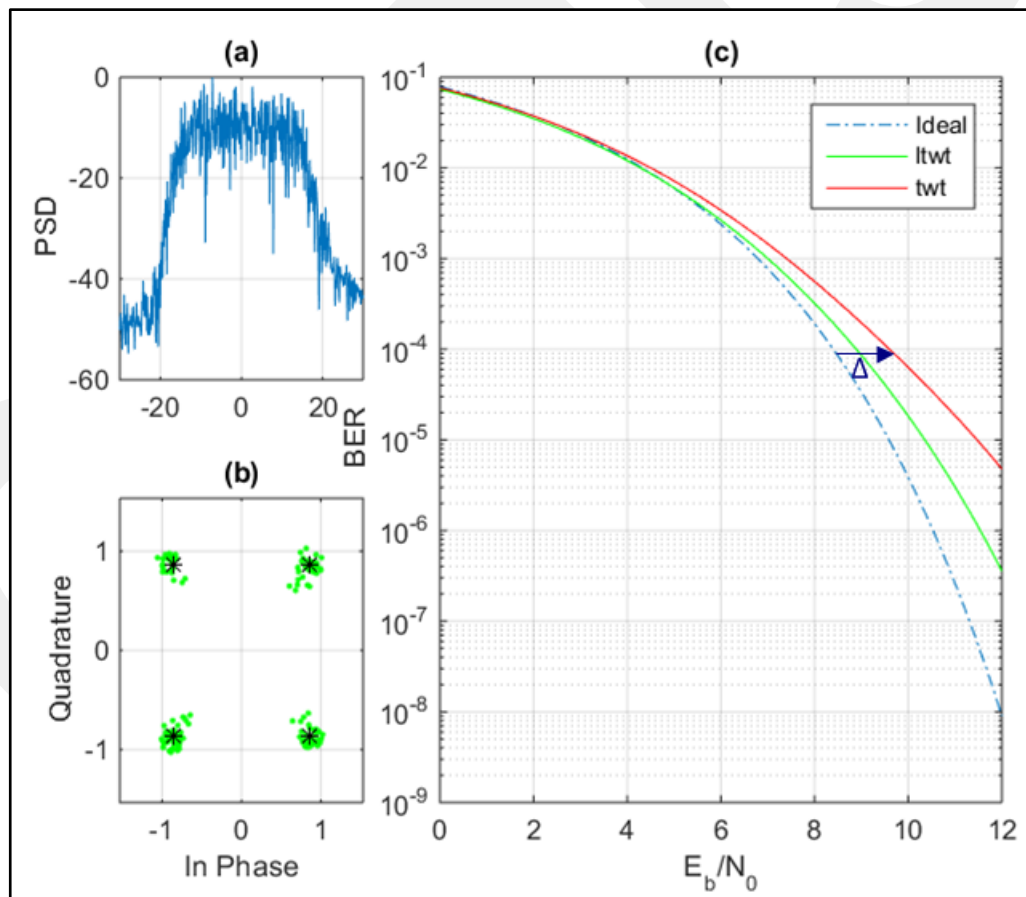


Figure 18 (a) PSD of carrier at OMUX out (b) Constellation (c) BER vs E_b/N_0

CHAPTER 5

RESULTS AND DISCUSSION

As explained in section 3.2.1 and shown in Table 1, four carrier scenarios representative of actual transponder utilization are determined for studying in this thesis. Results associated with these scenarios are presented in following sections.

5.1. Single QPSK Modulated Carrier

A single 30MSPS QPSK carrier is simulated through the 36 MHz channel. This is a representative scenario for mainly DTH TV transmission. In addition, it can be considered as a forward channel for a data link even though usually higher modulation levels are tried to be utilized in such occasions.

Figure 19 and Figure 20 show the TD and its components with respect to IBO for the transponder model utilizing TWT and its linearized version LTWT respectively. For TWT case, Δ alone reaches 1.4dB at saturation. OBO_{mod} is determined from the AM/AM curve and modulation loss which is approximated as 0.33dB for QPSK. Optimal operating point where we can minimize TD is at -3dB IBO, where the TD is 1.4dB. For LTWT, optimal operating point moves towards saturation. A minimum TD of 1.2dB can be reached between a range of -2dB IBO and saturation.

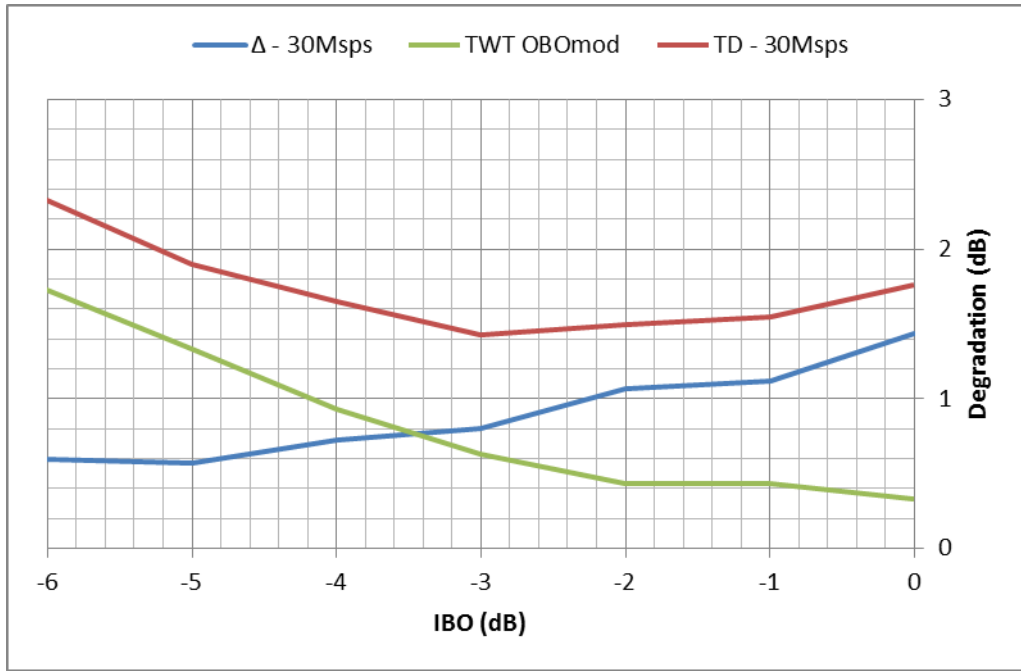


Figure 19 Total Degradation for 30Mps Single Carrier with TWT

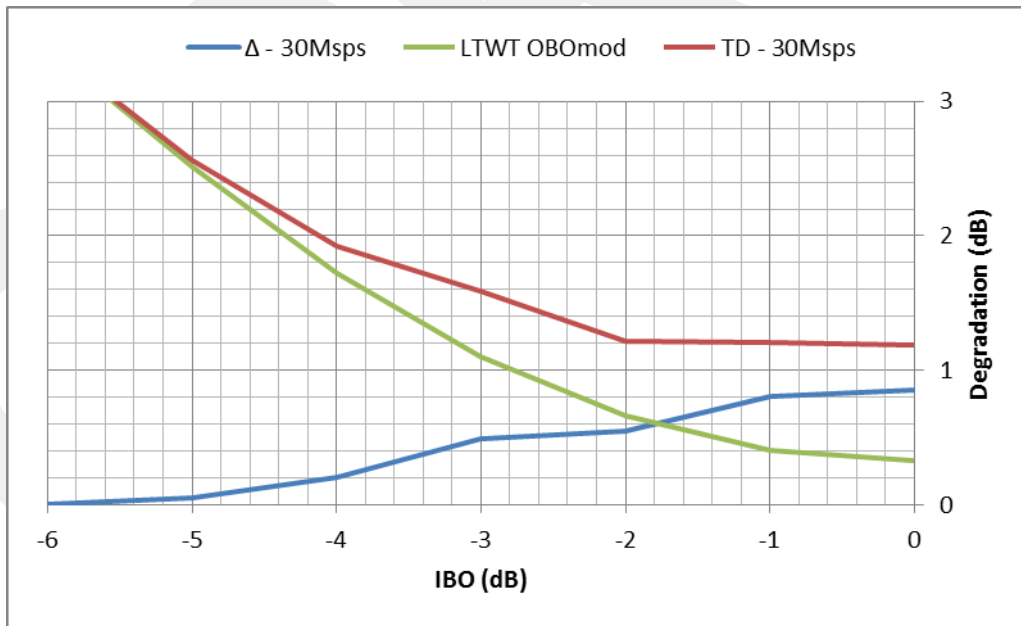


Figure 20 Total Degradation for 30Mps Single Carrier with LTWT

In single carrier mode of operation, it is beneficial to maximize symbol rate (SR) of the carrier for data transmissions by increasing the bandwidth towards guard bands between transponders even if there will be additional degradation because of filter rejection and group delay. This scenario is simulated and the TD results are presented in Figure 21 to decide on the maximum allowable SR.

Recalling that 20% roll-off is used in simulations, 38 Msp/s carrier has 45.6 MHz bandwidth and severely penalized by the IMUX and OMUX filters. However, other three are in 2dB range and additional data rate provided by higher SR can be benefited if the link has margin to allocate.

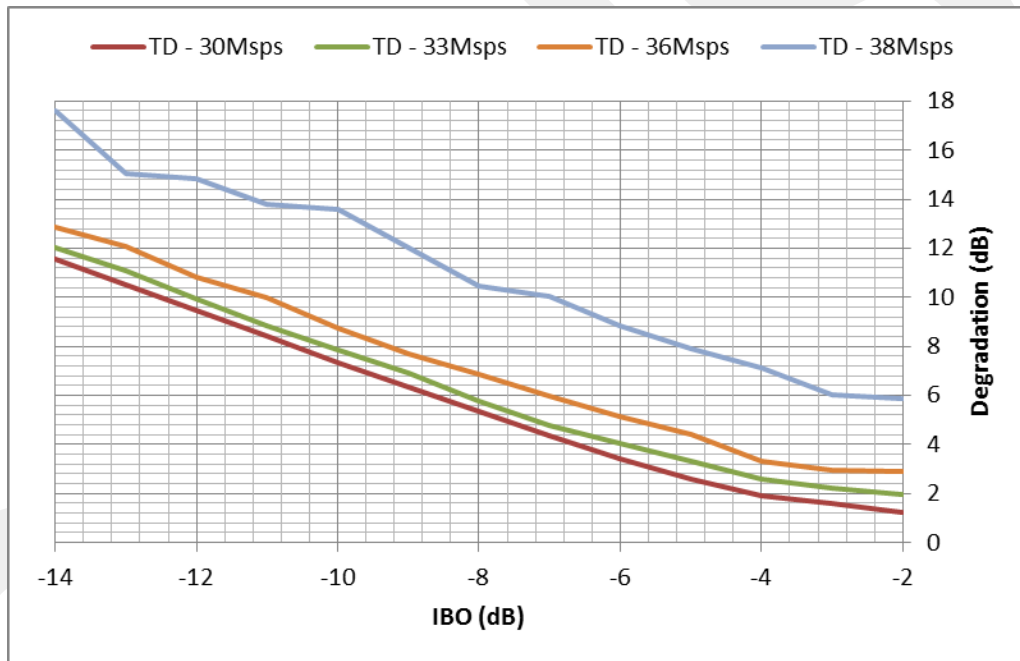


Figure 21 Total Degradation for a single carrier with varying symbol rate

5.2. Dual QPSK Modulated Carriers

Dual 14.8Msp/s QPSK carriers with 20% roll-off are simulated through the same 36 MHz channel. This is a representative scenario for data transmission in forward link. Figure 22 shows the results comparatively for each carrier and through TWT and LTWT.

When there is more than one carrier, the IM distortion starts to appear. TWT has to be operated at -6dB IBO and the minimum TD is 2.7dB. LTWT allows operating transponder around -2,-3dB IBO range with 1.8dB TD, improving the performance by 0.9dB.

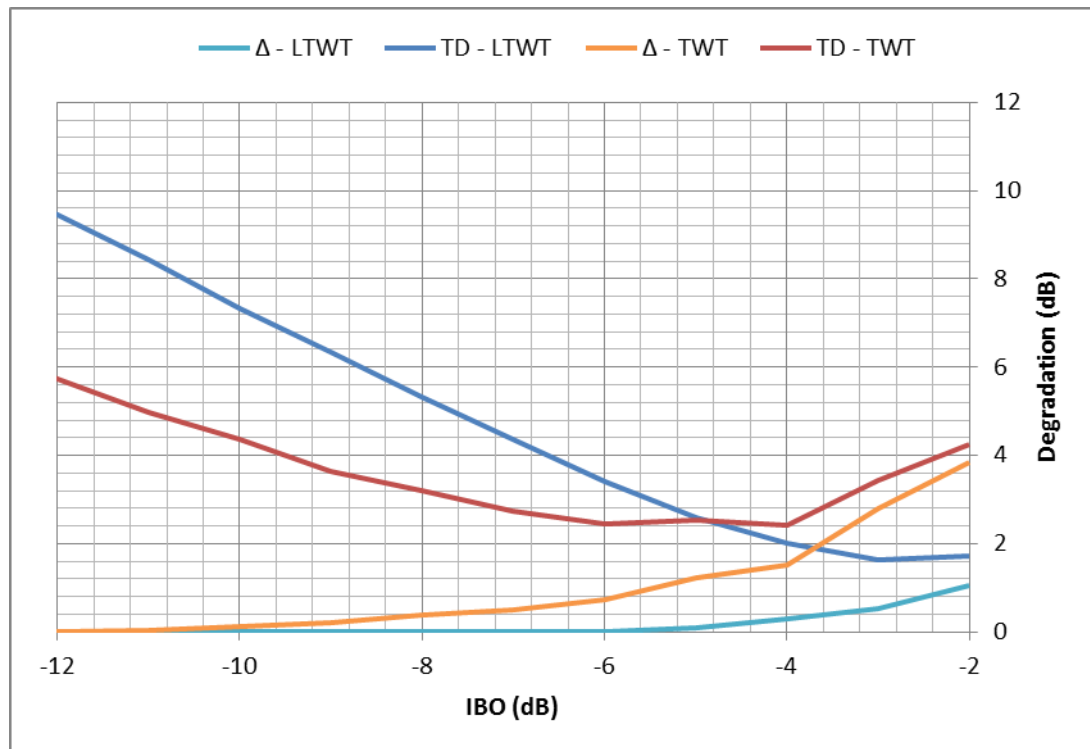


Figure 22 Total Degradation for dual 14.8 Msps carriers

5.3. Multicarrier Scenario with 8 QPSK Modulated Carriers

A multicarrier scenario has been prepared with 8 carriers each having 3.5Mpsps symbol rate and 20% roll-off. There is 300 KHz guard band among each carrier. This could be considered as a representative scenario for data transmission in return link. Figure 23 shows the Δ and TD results for Carrier #1 through TWT and LTWT. This carrier is placed at right hand side of the center frequency.

As anticipated, with 8 carriers, IM distortion is severe when operating close to saturation. This scenario is the one where the maximum benefit from the linearizer is expected. Consistently, we observe that the Δ is 0dB until -6dB IBO for LTWT

whereas it starts rising at -12dB IBO for TWT. However, if we only compare IBO, it is possible to judge the benefit of linearizer optimistically since when the actual degrading factor of OBO corresponding to the given IBOs are considered, the benefit is not that high. TWT has to be operated at -9dB IBO and the minimum TD for this carrier is 4.7dB. Optimum operating range for LTWT is at [-5,-4] dB IBO range with 3.2dB TD which provides 1.5dB performance improvement compared to TWT case.

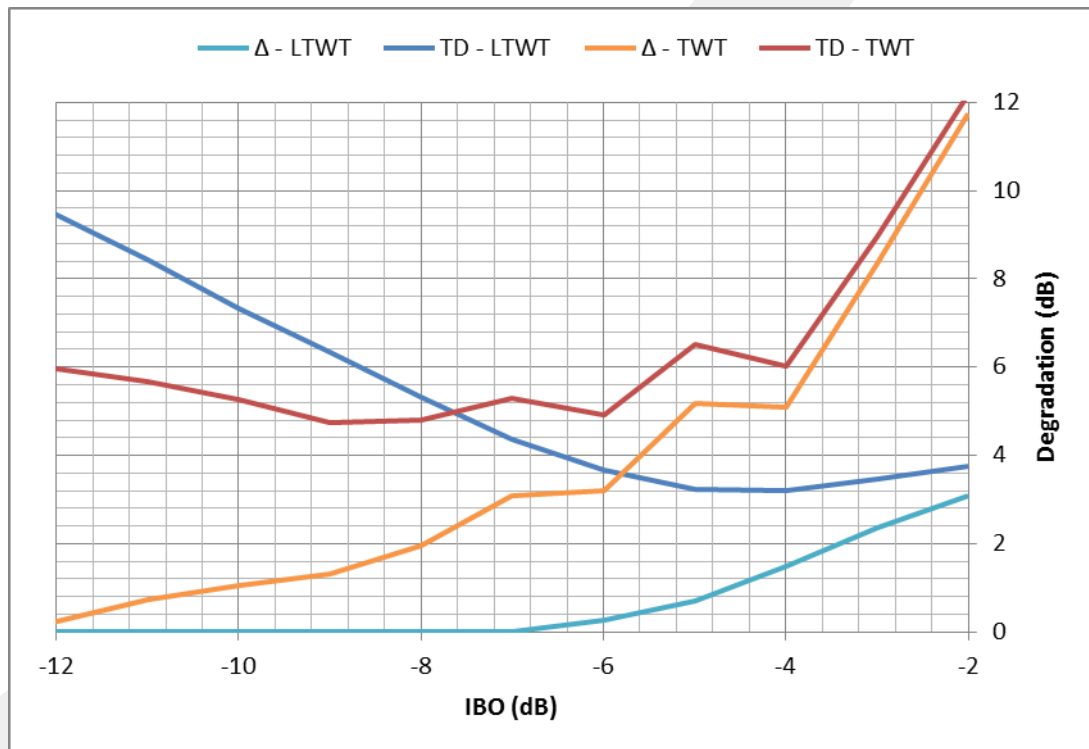


Figure 23 Total Degradation for multicarrier scenario with 8 carriers

All above studies have been implemented with sufficient guard band among carriers however for capacity maximization it may be necessary to bring carriers very close to each other e.g. for frequency planning of multicarrier return link use. In such a practice, the impact of ACI is a decisive factor. In a multicarrier system, adjacent channel's power will be captured by the receiver causing ACI [6]. The wider the guard band between carriers, the smaller is the adjacent channel power however wider guard bands decrease efficiency. For above scenario of 8 carriers, ACI is studied by decreasing the guard band between carriers as visualized in Figure 24.

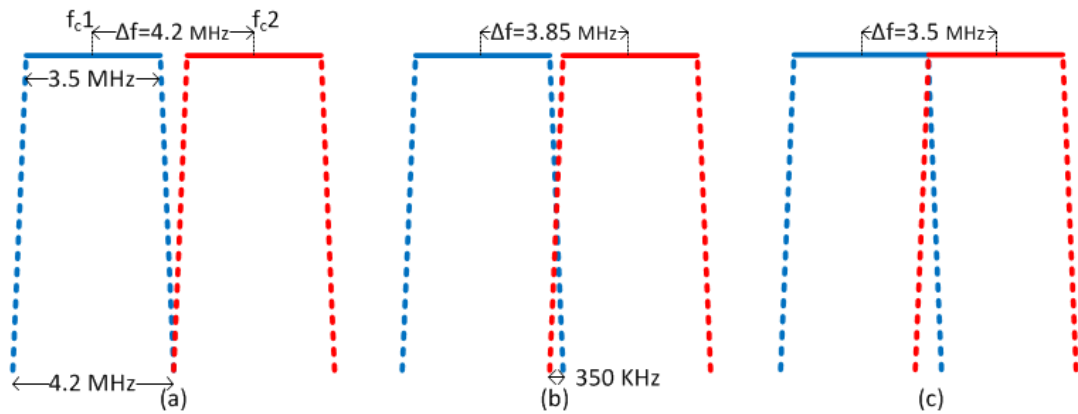


Figure 24 ACI analysis for two 3.5Mps carriers with varying separation (a) $\Delta f=4.2$ MHz, (b) $\Delta f=3.85$ MHz, (c) $\Delta f=3.5$ MHz,

The study have been performed at perfectly linear region for LTWT (-20 dB IBO) in order to eliminate other non-linear degradations. Therefore the degradation measured in this scenario is totally due to ACI and we will call it Δ ACI. The initial guard band was 300 KHz and corresponding center frequency separation (Δf) is 4.5 MHz between two carriers. Results are presented in Figure 25.

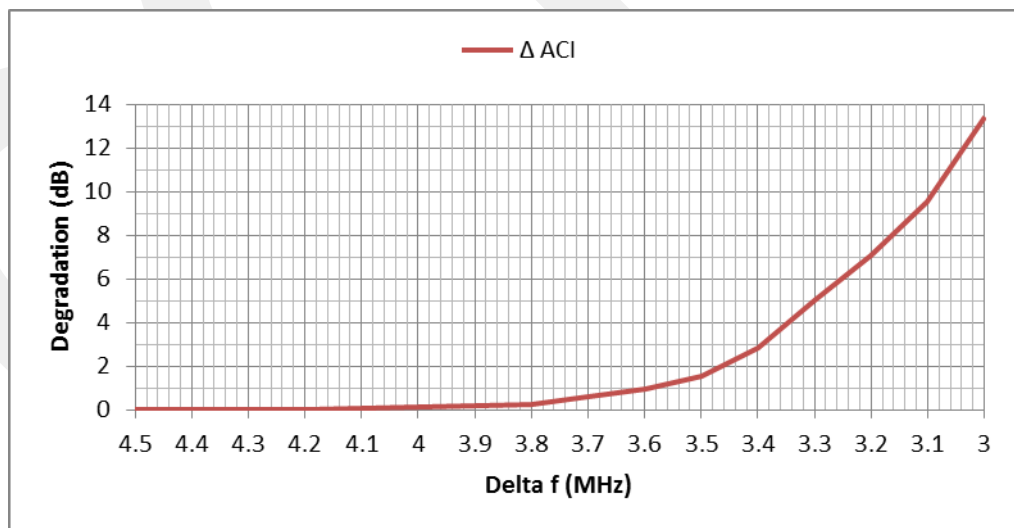


Figure 25 ACI analysis degradation curve

When the two carriers just touch each other as visible in Figure 24(a) there is not any degradation. 350 KHz carrier skirt overlap as seen in Figure 24(b) can be tolerated

with a degradation of 0.2dB where Δf is 3.85 MHz. After this point carriers are over each other and degradation curve ramps up. From these results, we can conclude that for carriers with the same SR and roll-off, skirt overlap corresponding to a Δf value of $(SR*(1+roll-off/2))$ is the minimum tolerable separation causing quite low degradation, i.e. 0.2dB. However, we have to note that, the decision of Δf should also take into account the actual earth station receiver characteristics and transmitter frequency stability.

5.4. Single Carrier Scenario with Various Modulations

After detailed investigation of simulation results with QPSK modulation for various scenarios, this section provides the results for higher modulation schemes for single carrier usage. Figure 26 show the AWGN BER performances of 8PSK, 16APSK, 32APSK, 64APSK and 256APSK modulations without coding. Please note that an analytic BER calculation is possible only for 8PSK modulation and it is given in the figure along with simulation result called '8PSK SC BER'. Here SC is used to indicate short circuiting of simulated transponder to have an AWGN representative simulation environment as explained in section 3.3. Therefore SC represents the results obtained with simulation for AWGN performance.

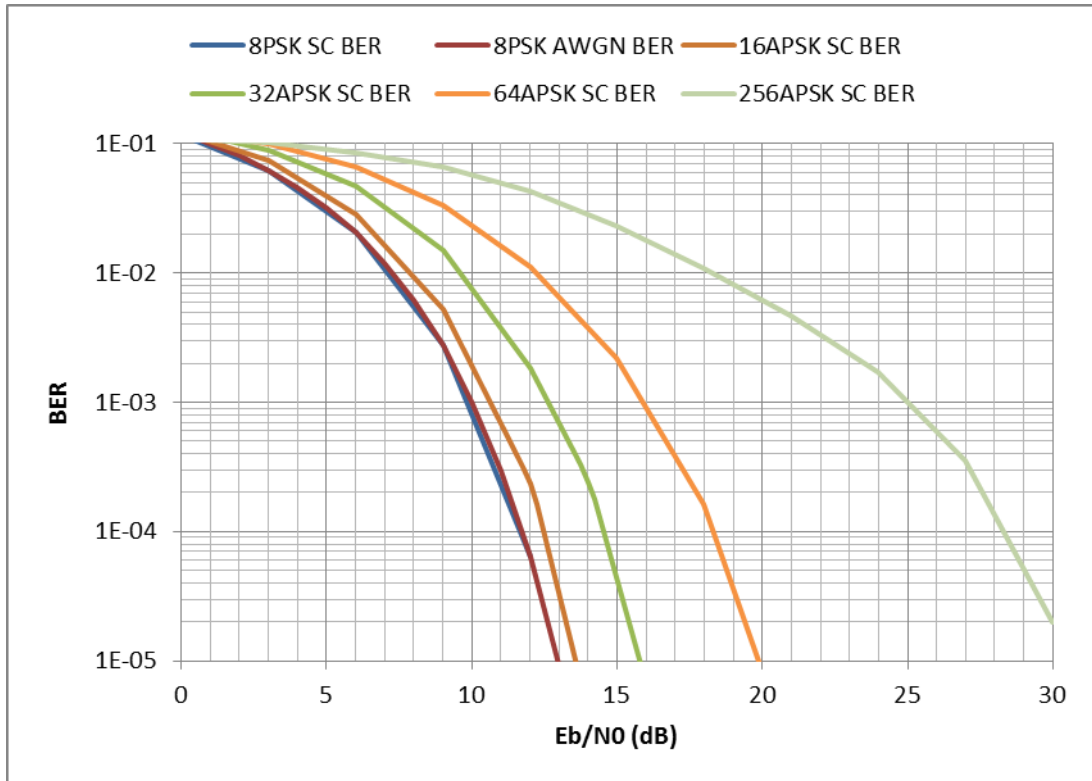


Figure 26 Uncoded AWGN BER Performances of 8PSK and M-APSK Modulations

For APSK modulation schemes theoretical AWGN performances are not available and only simulated performances are presented. The extra power demand of the higher modulation schemes is quite immense as visible. 64 and 256APSK modulations, recently introduced by draft DVB-S2X standard [2] are especially too demanding that they may have very rare utilization in future, possibly only for point to point applications with large size antennas. These recent modulations are also very prone to transponder non-linearities and they suffer severe degradation. Therefore, a comparison of Δ caused by satellite transponder for 8PSK, 16APSK and 32APSK which have currently been utilized in satellite communications are characterized and presented in Figure 27. Δ for single QPSK carrier which has already been presented previously is added in the graph for comparison.

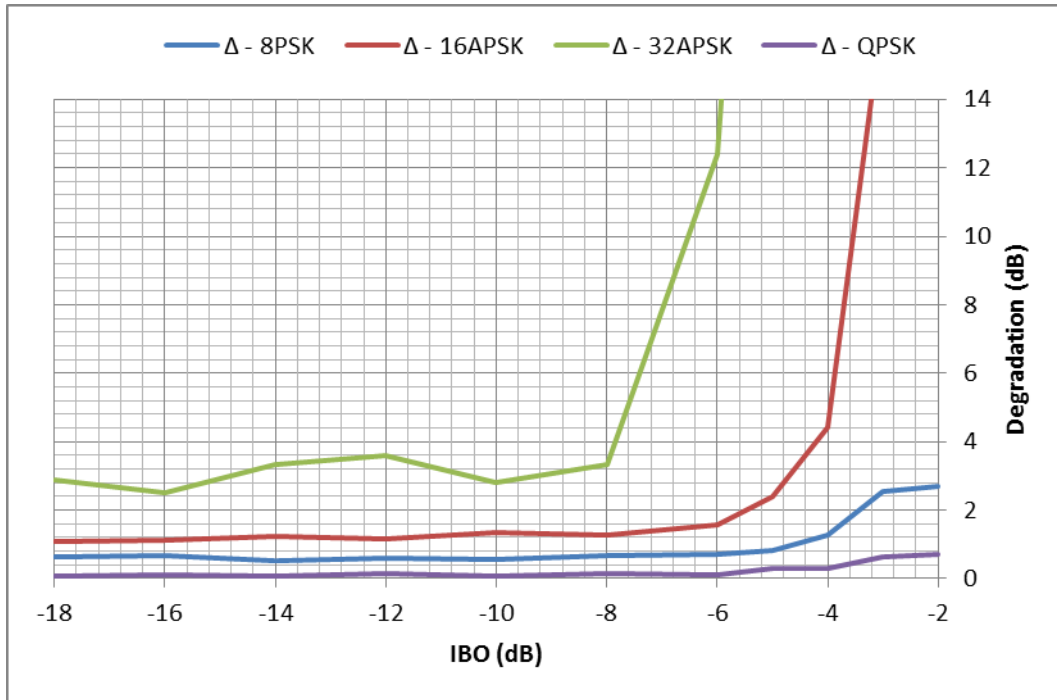


Figure 27 Degradation (Δ) for QPSK, 8PSK, 16APSK and 32APSK Modulations

Figure 27 clearly identifies that higher modulation schemes of 16APSK and 32APSK are demanding linear transmission environment much more than QPSK and 8PSK modulations. Otherwise they suffer too much degradation. Optimum operation point of each modulation, in single carrier scenario for the simulated T3A LTWT can be extracted from above figure as the lowest degradation point close to saturation. These are identified in Table 2.

Table 2 Optimum Operation Points wrt. Modulation for Simulated LTWT

Modulation	IBO (dB)	OBO (dB)	Degradation (Δ) (dB)
QPSK	-2	0.66	0.7
8PSK	-4	1.72	1.3
16APSK	-6	3.4	1.6
32APSK	-8	5.3	3.3

When we compare different modulations, the price of higher bandwidth efficiencies provided by higher modulations are not free at all. In the satellite network analysis, a

comparison of different modulations by just looking at the AWGN E_b/N_0 requirements will produce optimistic results in favor of higher modulations. The necessary back off levels and the degradation have to be used in conjunction with AWGN performances in order to have a realistic performance comparison.

In order to have a further validity check of the simulated performance as represented above, non-linear degradation test data provided by a satellite ground station equipment manufacturer [21] is compared with the simulation results as shown in Table 3.

Table 3 Comparison of Simulated Performance with a Manufacturer's Data

Modulation	Simulation Results			Manufacturer Data	
	IBO (dB)	OBO (dB)	Degradation (Δ) (dB)	OBO (dB)	Degradation (Δ) (dB)
QPSK	-2	0.66	0.7	0.7	0.65
8PSK	-4	1.72	1.3	0.7	1.18
16APSK	-6	3.4	1.6	1.6	2.41
32APSK	-8	5.3	3.3	4.5	2.56

It has to be noted that there are many factors those can potentially cause different level of degradations among the simulation and test data. For instance, provided test data is obtained for single carrier utilization of a different satellite transponder for which the specifications are not available. In addition, the carrier used in testing has FEC implementation unlike the simulation. Lastly, such testing through real satellite link introduces additional inaccuracy because of atmospheric and interference impacts which cannot be avoided in real satellite link. Therefore, it is not expected to have a one to one correspondence in the comparison table. Actual intention is to have a sanity check of the simulation results.

When the simulation and test data is compared, similar kind of behavior is observed but test results are more optimistic. This is in line with expectations because the tests have been performed with coded signals and coding decreases the level of

degradation up to a certain extent. In conclusion, similarity with test results proves the validity of the simulation.

5.5. Link Budget Calculations and Optimization of Transponder Utilization

So far in this chapter the simulation results are presented and the total degradation figures caused by transponder non-linearities and filtering impacts are characterized for various scenarios. Once such degradation values are at hand, we now turn our attention to optimize the transponder utilization, i.e. find the optimal operating point of the transponder in order to obtain the best link performance. One may think that the IBO corresponding to the lowest TD figure provides the best link margin. It certainly provides a trustworthy estimation however it is not hundred percent true as it will be demonstrated through examples after a brief introduction of satellite link budget calculations.

Typically frequencies from 1 to 40 GHz are used in satellite communications. For both uplink and downlink carriers at such high frequencies, several impairments of the atmosphere are induced degrading the performance of the communication link. Rain causes severe attenuation especially above 10 GHz which is the worst loss caused by atmosphere to the radio waves which have to be taken into account while designing the satellite link. For the purpose of our discussion though, clear sky conditions are assumed because our aim is to find out the impact of transponder degradation to overall link which is irrelevant of rain and other atmospheric attenuations.

References [4, 6 and 8] define the complete contributors of a satellite link budget. For brevity final formulas involved in link budget calculations are going to be provided here.

For an individual satellite uplink or downlink C/N_0 is given by the following formula [6];

$$L_{FS} = (4\pi R/\lambda)^2 \quad (22)$$

$$\frac{C}{N_0} = EIRP \left(\frac{1}{L_{FS}} \right) \left(\frac{G}{T} \right) \left(\frac{1}{k} \right) \quad (Hz) \quad (23)$$

L_{FS} is called free space loss and represents the ratio of the received and transmitted powers in a satellite link. λ is wavelength and R is the distance between the earth station and the satellite. Since communication satellites are around 36000 Km away from the earth stations, the free space loss is around 200 dB in one direction for Ku band. C/N_0 is carrier to noise power spectral density and k is the Boltzman constant (-228.6 dBW/HzK). G/T and EIRP were defined by equation (1) and (2) respectively. Equation (23) shows that one way link performance depends on EIRP of transmitting station, the free space loss in between the two terminals and G/T of receiving station. For the uplink, transmitting station is the earth station and receiving station is the satellite. Therefore, EIRP of earth station and G/T of satellite are taken into account in uplink calculation. For the downlink the situation is vice versa of the uplink, this time EIRP of the satellite and G/T of the receiving earth station are used. In linear scale C/N_0 is obtained in Hz. Usually dB convention is used in satellite link budgets and C/N_0 is represented in dBHz by calculating $10 \cdot \log_{10}(C/N_0)$.

Total link which is the combination of uplink, transparent satellite transponder impact and downlink is given by the following formula [6]:

$$\left(\frac{C}{N_0} \right)_T^{-1} = \left(\frac{C}{N_0} \right)_U^{-1} + \left(\frac{C}{N_0} \right)_D^{-1} \quad (Hz) \quad (24)$$

where T stands for total link, U stands for uplink and D stands for downlink. Above formula can be modified by addition of intermodulation and interference impacts to obtain a more general term [6]:

$$\left(\frac{C}{N_0} \right)_T^{-1} = \left(\frac{C}{N_0} \right)_U^{-1} + \left(\frac{C}{N_0} \right)_D^{-1} + \left(\frac{C}{N_0} \right)_I^{-1} + \left(\frac{C}{N_0} \right)_{IM}^{-1} \quad (Hz) \quad (25)$$

where $\left(\frac{C}{N_0}\right)_I$ is carrier power to interference noise power spectral density ratio and $\left(\frac{C}{N_0}\right)_{IM}$ is carrier power to intermodulation noise power spectral density ratio. Finally, C/N is easily obtained by the following formula [6];

$$C/N \text{ (dB)} = C/N_0 \text{ (dB)} - BW \text{ (dB)} \quad (26)$$

where BW is the noise bandwidth of the carrier.

Satellite link budget calculations can conveniently be performed with a spreadsheet like the one presented in Appendix A. This link budget tool is prepared and used to obtain the results provided in the following sections. It also displays the step by step calculations and the formulas used in a more comprehensive manner than the brief summary provided in this section.

5.5.1. Dual Carrier Scenario Link Budget Calculations

The simulation results of dual QPSK carrier scenario were presented in section 5.2 showing degradation Δ , OBO_{mod} and TD. Now we are going to use these results in the link budget calculations as described below and try to determine optimal link performance taking into account simulated degradation figures as it is our ultimate purpose:

- Calculations are performed for both TWT and LTWT. Related Δ and OBO_{mod} figures are used in each case.
- For each IBO value, the associated OBO_{mod} is incorporated in link budget calculations as transponder OBO value.
- For each IBO value, the associated Δ is added to the link threshold level defined for linear channel. These threshold levels could be obtained from DVB standards for each modulation/coding pair which are defined in E_b/N_0 or E_s/N_0 figures. However, in order to have a more realistic figure, a satellite ground station equipment manufacturer's data [21] is preferred which

reflects actual hardware performance including receiver implementation margins.

- Since the intermodulation degradation caused by satellite transponder is accounted in Δ figure, link budget tool's $C/IM_{\text{satellite}}$ term is taken as 200dB in order not to degrade the link twice by the same impairment. Please note that, if one tries to make link budget calculations without having such degradation results, transponder C/IM3 performance is used to account for intermodulation distortion. Such calculations using C/IM3 performance of the satellite is also going to be provided for comparison.
- Same situation is valid for C/ACI (Carrier to Adjacent Channel Interference Ratio) and it is taken as 200dB in link budget tool.
- Calculations are performed using a QPSK 5/6 FEC scheme. Associated threshold E_s/N_0 level is used as mentioned above.
- For each carrier, symbol rate is 14.8 Msps, roll-off is 20% and bandwidth is 17.6 MHz as defined previously and as simulated. Transponder bandwidth is 36 MHz.
- A 3.7m U/L antenna is assumed. On downlink site, calculations are performed for 60cm, 90cm and 2.4m antennas. 60cm and 90cm antennas represent either DTH TV reception antennas or VSAT remote terminal antennas for data link.

Following above methodology, total link $C/(N+I)$ is calculated using the spreadsheet link budget tool. Here the interference term includes typical ASI (Adjacent Satellite Interference) and XPI (Cross Pole Interference) terms but ACI and C/IM3 has negligible impact since we are using 200dB values for them as explained above. Finally, the link margin (LM) is calculated by:

$$\text{Link Margin}(dB) = C/(N + I)_t(dB) - [\text{Linear Ch. treshold } E_s/N_0(dB) + \Delta(dB)] \quad (27)$$

where $C/(N + I)_t$ is the total link carrier to noise plus interference ratio and equals to the E_s/N_0 , linear channel threshold E_s/N_0 is read from the data sheet as explained and Δ is the degradation obtained by the simulation. $C/(N + I)_t$ is calculated by

assuming there is not any degradation occurring through the transponder i.e. the transponder is truly linear. It just incorporates the OBO_{mod} value associated for each level of IBO. The linear channel threshold E_s/N_0 is increased by the amount of simulated Δ to take into account the transponder degradation and the difference is the link margin which takes into account whole link and transponder performance including non-linearities and filtering distortions.

Let us start examining the link budget calculation results by 60cm Rx antenna as presented in Figure 28. If we compare this figure with Figure 22, we may recall the four lines at the bottom of the figure, representing Δ and TD performances for the dual carrier scenario. Now the top two lines are added representing calculated link margin for LTWT and TWT.

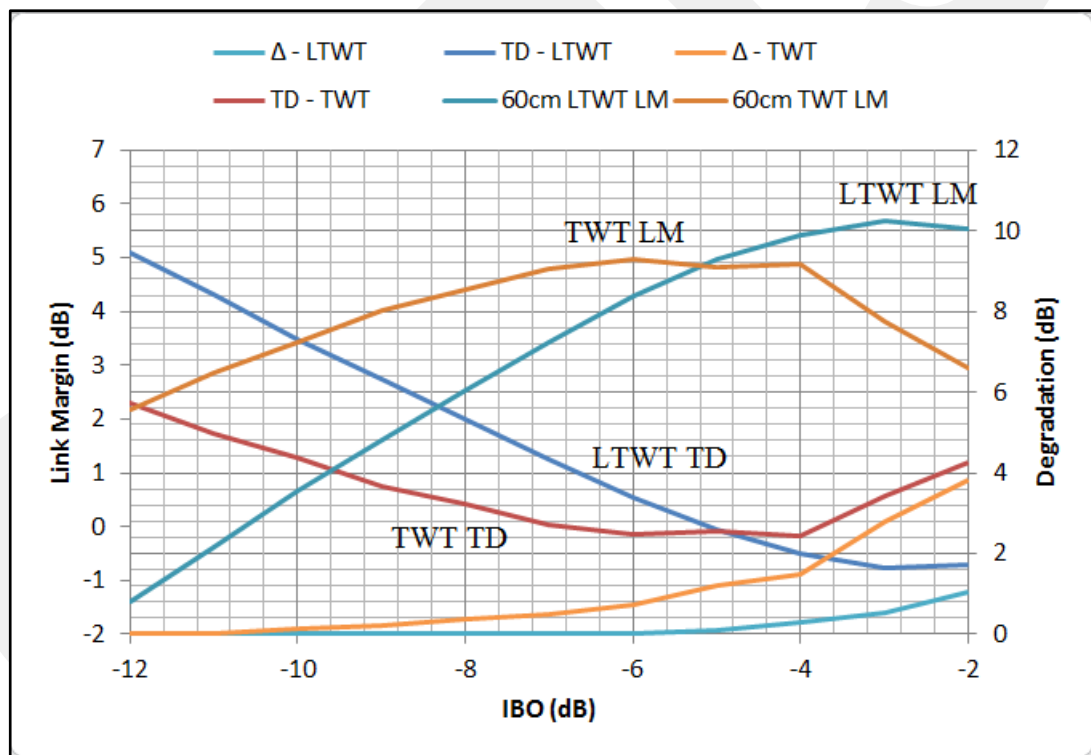


Figure 28 TD and 60cm Antenna Link Margin for Dual Carrier Scenario

The horizontal symmetry between TD and LM curves are visible. This suggests that the TD curves can be used to determine the optimal operating point for this carrier scenario when the Rx antenna is 60cm. In other words, lowest TD corresponds to

maximum link margin. Numeric figures for optimum performance are summarized below:

- TWT: Min TD = 2.7dB @ -6dB IBO; Max LM = 4.98dB @ -6dB IBO
- LTWT: Min TD = 1.8dB @ -2,-3dB IBO; Max LM = 5.69dB @ -3dB IBO

The link budget is also calculated for 90cm and 2.4m antennas and resulting LM curves are presented in Figure 29.

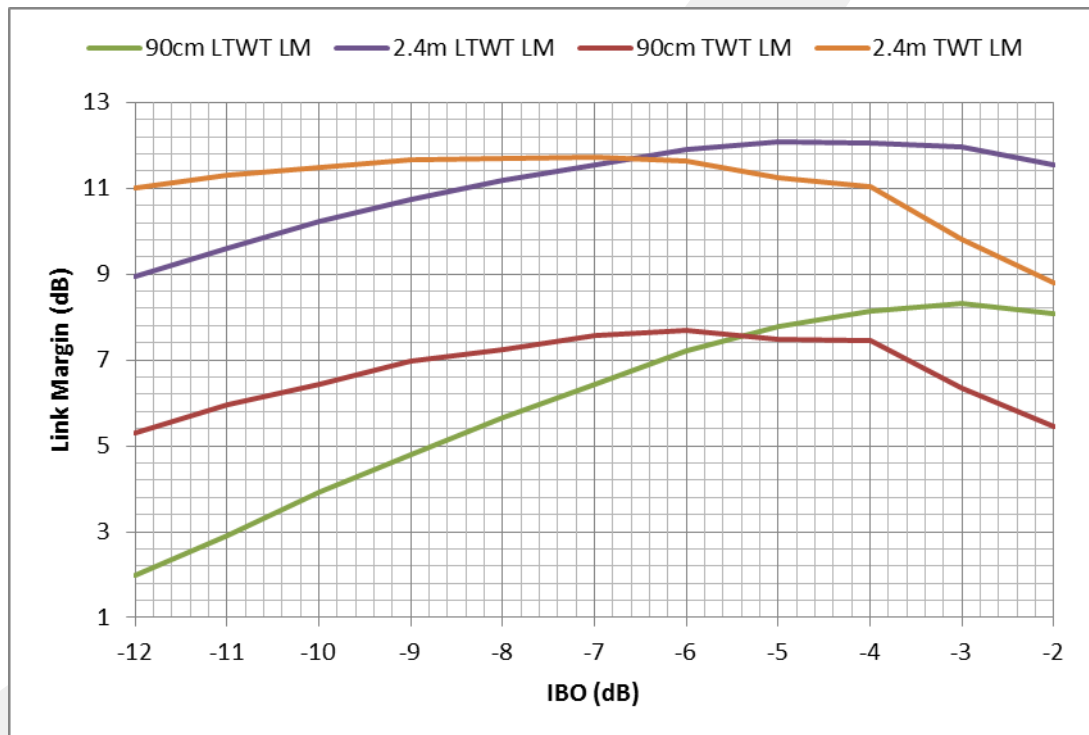


Figure 29 Link Margin for Dual Carrier Scenario – 60cm and 2.4m Rx Antennas

The couple of lines on top of the figure belong to 2.4m antenna and the bottom couple belongs to 90cm antenna. We observe similar behavior for 90cm antenna like the 60cm antenna in terms of optimum operating points i.e. -3dB for LTWT and -6 dB for TWT. On the other hand, for 2.4m antenna optimum operating point moves down to -5dB IBO for LTWT and -7dB IBO for TWT where the transponder is more into linear region. These results are summarized in Table 4 below:

Table 4 Optimum Performance Comparison for Dual Carrier Scenario

Ant. Size	TWT				LTWT				LM Diff. (dB)	Δ Diff. (dB)	TD Diff. (dB)
	IBO(dB)	LM(dB)	Δ (dB)	TD(dB)	IBO(dB)	LM(dB)	Δ (dB)	TD(dB)			
60cm	-6	4.98	0.73	2.46	-3	5.9	0.54	1.64	0.92	0.19	0.82
90cm	-6	7.69	0.73	2.46	-3	8.31	0.54	1.64	0.62	0.19	0.82
240cm	-7	11.74	0.49	2.72	-5	12.07	0.08	2.6	0.33	0.41	0.12

In Table 4, link margin, Δ and TD performance differences between TWT and LTWT are calculated for the IBO level where the link margin is maximized. Δ and TD difference values between the TWT and LTWT corresponds to improvement introduced for this carrier scenario by the linearizer. LM differences depend on the antenna size in addition to the linearizer improvement. We observe that, the smaller the receive antenna is, the most benefit obtained from the linearizer in terms of link margin because the link margin difference between LTWT and TWT is 0.92 dB for 60cm antenna whereas it drops down to 0.33dB for 240cm antenna. This is actually caused by the satellite link dynamics. It is always desirable for logistics and cost reasons to have smaller Rx antennas but they have lower gain and they need the satellite transponder to be driven as close as saturation to get the highest EIRP available. Linearizer comes into game here and it provides better linearity close to saturation compared to TWT alone. Bigger antennas, on contrary, have higher gain and they can tolerate more back-off in order to get less degradation caused by the transponder. The increase in back-off increases the linearity of the TWT and the performance improvement coming from the linearizer diminishes.

Regarding dual carrier scenario, a final performance comparison with a 60cm antenna between link budgets incorporating simulation results as presented above and link budgets using C/IM3 and NPR is presented in Figure 30. Performance comparison is prepared for LTWT. While calculating link margin with C/IM3 performance, for each IBO value, corresponding C/IM3 performance is used as given in Figure 5 in link budget tool's $C/IM_{\text{satellite}}$ term. Similarly, NPR performance is used as given in Figure 7 to calculate link margin with NPR. Since we are incorporating non linearity in link budget calculation either with C/IM3 or NPR performances, threshold levels are not modified and the thresholds given for linear channel is used.

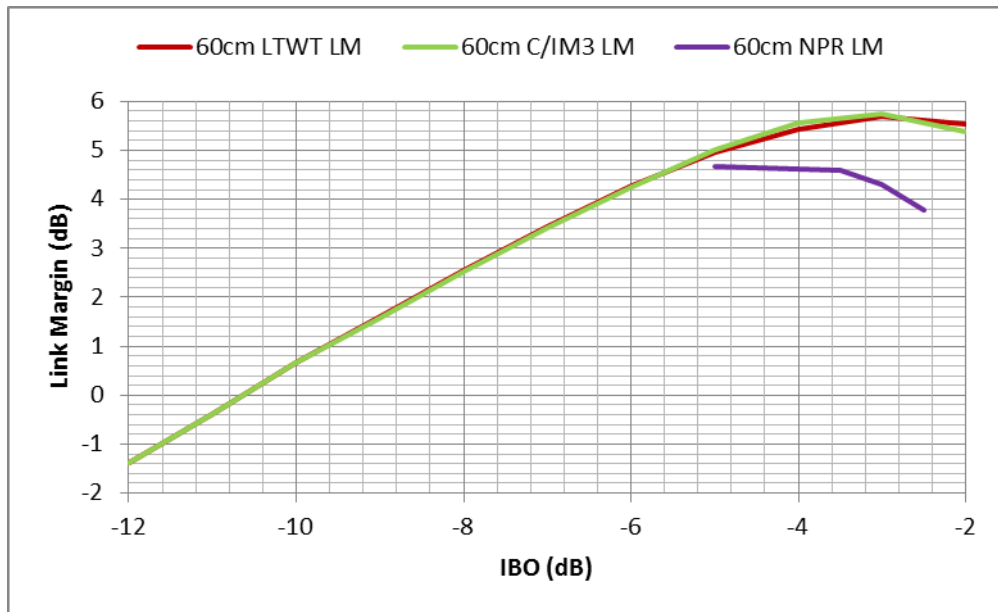


Figure 30 Link Margin Comparison for Dual Carrier Scenario – TD, C/IM3 and NPR

Looking at Figure 30, we can see that the link margin obtained with simulation results and the link margin incorporating C/IM3 performance overlap. However, NPR calculation produces more pessimistic results. This is in line with our expectations because C/IM is measured with two unmodulated carriers and NPR represents the performance when there are many carriers over the transponder. The simulation results, on the other hand, does not only account for intermodulation distortion but also phase distortions and filtering impacts. We see that these other impacts are negligible for dual QPSK carrier scenario and intermodulation distortion is the determining factor. By the way, NPR results are unfortunately available just for a few IBO levels only and therefore it was not possible to produce whole IBO range results for NPR case.

5.5.2. Multicarrier Scenario with 8 QPSK Modulated Carriers Link Budget Calculations

Similar to dual carrier case, link budget calculations are performed using simulated TD performance of 8 QPSK modulated carriers. This time, for briefness only a comparison with C/IM3 and NPR performances are presented in Figure 31, again for a 60cm Rx antenna.

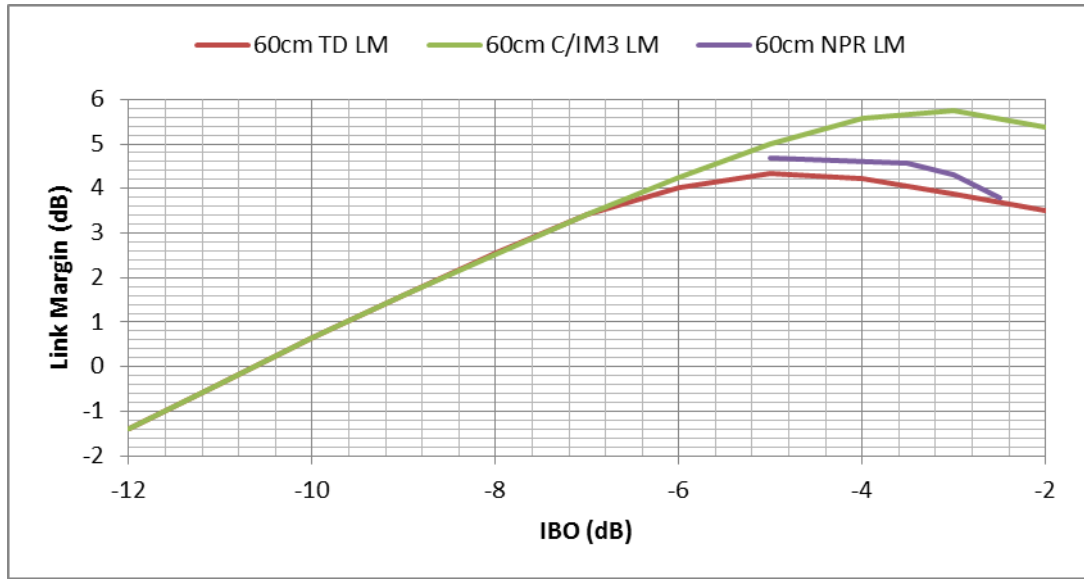


Figure 31 Link Margin Comparison for 8 Carriers Scenario – TD, C/IM3 and NPR

The C/IM3 and NPR curves are actually the same as dual carrier scenario since they incorporate measured LTWT C/IM3 and NPR performances which are irrelevant of the studied carrier scenario. However, the difference of link margin with TD performance curve is evident. This time TD link margin curve is far away from the C/IM3 curve and it is close or even lower than the NPR. This result is also in line with the expectation since 8 carrier simulation aims to demonstrate the distortion as severe as faced with NPR case. The TD curve is lower than NPR curve at some points since it incorporates all degradations caused by the transponder whereas NPR curve only accounts for the intermodulation distortion.

As we have seen the degradation figures are even worse when higher modulations such as 16APSK or 32APSK are utilized. Therefore, actual link margins that can be obtained with higher modulations will differ more from the ones obtained with basic C/IM3 and NPR performances.

5.5.3. Evaluation of Link Budget Calculations

Evaluating the combined link budget results with the degradation figures obtained with the simulation, the IBO corresponding to lowest TD point is not always the optimal operating point but it is a very good approximation which is valid in many cases. However, to be more precise, our assertion driven from the results is that, lowest TD point sets forth the upper IBO limit to be used in utilization of such scenario for which the exact optimal IBO level has to be determined with respect to downlink antenna size. If the D/L antenna size is very small (60cm-90cm), like a DTH TV reception antenna or VSAT remote terminal antenna, then the transponder should be operated at this upper bound. If the D/L antenna is a medium or big size professional one (>1.8m), then since it has more gain it can tolerate more back-off while benefiting from linearity more. So, optimal operating IBO decreases towards more linear region.

Following the methodology presented in this section, one can determine the optimal operating point and precise link margin for any scenario using the simulation results. Compared to regular link budget calculations, this method provides more accurate and unambiguous results since the transponder degradations are totally captured in Δ obtained with simulation.

CHAPTER 6

CONCLUSIONS

Communication satellites are continuing to be an integral part of today's wireless world. With lots of unique advantages such as broadcasting ability from one satellite source to almost one third of the earth and limitless number of viewers and not requiring any terrestrial network infrastructure to provide broadband access everywhere; satellite communication is not only a complementary technology to terrestrial and wired networks but it also challenges them. Industry experts assert that by the year 2020 Terabit/s satellites are deemed feasible [22]. On the other hand, the expensive nature of space technology necessitates detailed planning of a satellite network before implementation and optimization of satellite utilization when the satellite is in orbit to provide the most cost effective solution.

Satellite link budget tools are used to characterize the uplink and downlink earth segment requirements based on a defined satellite performance, as well as to calculate the total throughput of the system. While recent DVB-S2X standard defines modulations up to 256APSK to increase the efficiency of the satellite networks, the degradations caused by the satellite transponders' non-linearities and filtering impacts which are especially critical for higher modulations are not captured by regular link budgets. Link budget tools depend only on the regular tests applied during manufacturing process of the satellites. C/IM3 and NPR performances are measured during manufacturing process, for instance, and they are then used in link budget calculations to make an assessment on intermodulation degradation. However with varying carrier number and modulations, it is hard to precisely characterize the performance. In addition, there is no way to incorporate filter performances and distortions caused by them in a basic link budget tool.

To overcome this problem, a satellite simulation tool based on actual test data of TURKSAT-3A satellite has been prepared. For this purpose, measured AM/AM and AM/PM responses of a TWT and its associated LTWT is used to model their behavior at the core of the transponder. IMUX and OMUX filter responses are modeled by constructing their impulse responses from amplitude and group delay

measurements. Input carrier modulation waveforms are prepared in line with DVB standards. BER analysis has been performed at the output of the simulation. By this tool, any multicarrier scenario utilizing modulations defined in DVB-S, S2 or S2X standards can be studied over the simulated transponder. It is possible to perform analysis for varying symbol rates, carrier numbers, carrier center frequencies, guard bands, carrier levels, IBO levels etc. which makes it possible to characterize any practical carrier scenario used in actual satellite communications. The output of the simulator is total degradation assessment which could directly be incorporated into link budget calculations. Such a tool is beneficial for capacity planning, performance assessment, specification evaluation for new satellites as well as educational purposes.

In the literature there has been extensive work performed to characterize the impact of TWT non-linearity on the communication performance [12, 15] or to analyze the benefit of adopting linearizers in satellites [10, 11]. There are also studies trying to make an assessment on overall satellite link performance [5, 14]. With regards to the difference of this thesis study from previous works, the test data coming from the manufacturing process is incorporated in the simulation instead of depending only on built in standard models, in order to characterize the performance of an actual satellite transponder. While there are very few studies performed on recently introduced DVB-S2X modulations, these are implemented in the simulation and compared with earlier modulations. TWT and LTWT are modeled separately and characterization of linearizer performance improvement has been performed for various scenarios. Dual and multicarrier analysis has been performed as opposed to single carrier case and impact of adjacent channel interference in multicarrier use is assessed. Finally, obtained degradation results are used in link budget calculations and complete link performance is evaluated to optimize transponder utilization.

An important result determined from the carrier scenarios studied is the dramatic increase in degradation figures with respect to modulation order, especially 16APSK and higher. It is shown that, not only the threshold E_s/N_0 requirements, generally provided for AWGN linear channel is sufficient for performance comparison of different modulations but also TD has to be taken into account. A trending solution for this problem is actually hidden inside the satellite transponder. As performance

enhancement of the linearizer for space TWTs are proven with comparative studies by this thesis, new satellite ground station hardware technologies are emerging to utilize pre-distortion linearizers on ground for further improvement of the transponder linearity to make it more suitable for higher modulations.

An aspect of this study to be developed as future work could be to model the complete satellite link incorporating a linearizer on ground and characterize the benefit provided by this additional linearizer. In addition, forward error coding algorithms defined by the DVB-S standards may be modeled for more precise performance estimation at each coding level.

REFERENCES

- [1] ETSI EN 302 307-1 V1.4.1 (2014-11), Digital Video Broadcasting (DVB); "Second generation framing structure, channel coding and modulation systems for Broadcasting, Interactive Services, News Gathering and other broadband satellite applications; Part 1: DVB-S2".
- [2] Draft ETSI EN 302 307-2 V1.1.1 (2014-10), Digital Video Broadcasting (DVB); "Second generation framing structure, channel coding and modulation systems for broadcasting, interactive services, news gathering and other broadband satellite applications; Part 2: DVB-S2 Extensions (DVB-S2X)".
- [3] W.H. Tranter, K.S. Shanmugan, T.S. Rappaport and K.L. Kosbar, Principles of Communication Systems Simulation with Wireless Applications. NJ: Prentice Hall, 2004.
- [4] D. Roddy, Satellite Communications, 4th ed. United States: McGraw-Hill, 2006.
- [5] E. Di Iorio, R. Ruini, V. De Nicola, A. Miglietta and R. Winkler, "End-to-end system performance evaluation in a forward and return satellite communications link," Satellite Telecommunications (ESTEL), 2012 IEEE First AESS European Conference on, vol., no., pp.1,6, 2-5 Oct. 2012.
- [6] G. Maral and M. Bousquet, Satellite Communications Systems, Systems, Techniques and Technology, 5th ed. Singapore: Wiley, 2009.
- [7] E.F. Nicol, B.J. Mangus, J.R. Grebliunas, K. Woolrich and J.R. Schirmer, "TWTA versus SSPA: A comparison update of the Boeing satellite fleet on-orbit reliability," Vacuum Electronics Conference (IVEC), 2013 IEEE 14th International , vol., no., pp.1,2, 21-23 May 2013.
- [8] International Telecommunications Union, Handbook on Satellite Communications (HSC), 3rd ed. Wiley, 2002.
- [9] X.T. Vuong, K.D. Nguyen, F.N. Ozmizrak and L.G. Birta, "Some practical strategies for reducing intermodulation in satellite communications," Aerospace and Electronic Systems, IEEE Transactions on , vol.24, no.6, pp.755,765, Nov. 1988.

- [10] A. Katz, R. Gray and R. Dorval, "Wide/Multiband linearization of TWTAs using predistortion," *Electron Devices, IEEE Transactions on*, vol.56, no.5, pp.959,964, May 2009.
- [11] A. Katz, R. Gray and R. Dorval, "Truly wideband linearization," *Microwave Magazine, IEEE* , vol.10, no.7, pp.20,27, Dec. 2009.
- [12] M. Aloisio, E. Casini and A. Ginesi, "Evolution of space traveling-wave tube amplifier requirements and specifications for modern communication satellites," *Electron Devices, IEEE Transactions on*, vol.54, no.7, pp.1587,1596, July 2007.
- [13] Young-Wan Kim, Yun-Jeong Song, Nae-Soo Kim and Dong-Chul Park, "Performance analysis of channel impairment in high data rate satellite communication service," *Microwave and Optoelectronics Conference, 2001. IMOC 2001. Proceedings of the 2001 SBMO/IEEE MTT-S International* , vol.1, no., pp.47,50 vol.1, 2001.
- [14] A. Ginesi, S. Cioni and M. Angelone, "DVB-S2X channel models: rationale and justifications," *Advanced Satellite Multimedia Systems Conference and the 13th Signal Processing for Space Communications Workshop (ASMS/SPSC), 2014 7th* , vol., no., pp.331,338, 8-10 Sept. 2014.
- [15] M. Aloisio, P. Angeletti, E. Casini, E. Colzi, S. D'Addio and R. Oliva-Balague, "Accurate characterization of TWTA distortion in multicarrier operation by means of a correlation-based method," *Electron Devices, IEEE Transactions on*, vol.56, no.5, pp.951,958, May 2009. Lei Cheng; Xinhai Tong; Jiuyin Wu and Bo Kong, "Analysis and simulation of HPAs' effects on satellite OFDM systems," *Information Science and Technology (ICIST), 2013 International Conference on*, vol., no., pp.1212,1216, 23-25 March 2013.
- [16] A. A. M. Saleh, "Frequency-Independent and Frequency-Dependent Nonlinear Models of TWT Amplifiers," *IEEE Transactions on Communications*, Vol. COM-29, No. 11, November 1981, pp. 1715–1720. ETSI EN 300 421 V1.1.2 (1997-08), Digital Video Broadcasting (DVB); Framing structure, channel coding and modulation for 11/12 GHz satellite services. M. C. Jeruchim, P. Balaban and K.S. Shanmugan, *Simulation of Communication Systems, 2nd Ed, Modeling, Methodology and Techniques*. New York: Kluwer Academic Publishers, 2002.

- [17] Proakis, J. G., Digital Communications, 4th Ed., McGraw-Hill, 2001.
- [18] <http://www.newtec.eu>/P. Inigo et. all, “Review of Terabit/s Satellite, the Next Generation of HTS Systems”, 2014 7th Advanced Satellite Multimedia Systems Conference and the 13th Signal Processing for Space Communications Workshop (ASMS/SPSC)

GCPRIS

Table 6 Link Budget Calculation – Outputs 1/2

OUTPUT 1/2			
UPLINK			
Transmit EIRP	66.03 dBW	$EIRP(dB)=HPA\ Power+Ant.\ Gain-Coupling\ loss$	
Transponder IBO	2.00 dB	User defined	
Defined Carrier IBC	5.07 dB	$=Txp\ IBO+10log(Txp\ BW/Carr\ BW)$	
Carrier IBO	5.07 dB	$=Txp\ IBO+10log(Txp\ BW/Carr\ BW)+(Req.\ EIRP-Tx\ El)$	
Antenna Mispnt	0.50 dB	User defined	
L free space	206.86 dB	$L=(4.\pi.R/\lambda)^2$	
Atmospheric absorp	0.11 dB	Parameters table	
C/N0u,thermal	97.16 dB/Hz	$C/N0u(dB)=EIRP-L+G/T-k-Ant.\ Misp-Atm.\ Abspt$	
C/Nu,thermal	25.46 dB	$C/N(dB)=C/N0-BW$	
C/(N+I)u	22.64 dB	$C/(N+I)^-1=C/Nu^-1+ C/ACI^-1+C/ASI^-1+C/XPI^-1+C/$	
Φ (PFD) carrier	-97.07 dBW/m2	$\Phi=EIRP-Ant.\ Misp-Atm.\ Abs.-10log(4.\pi.R^2)$	
Sat Rx Antenna Gai	42.69 dB		
P Rx @ Sat Rx Ant	-98.75 dBW	$P\ Rx=EIRP-Ant.\ Misp-Atm.\ Abs-L\ free\ space+G\ Rx$	
TOTAL ENDtoEND			
C/N0t,thermal	86.34 dB/Hz	$C/N0t^-1=C/N0u^-1 + C/N0d^-1$	
C/Nt,thermal	14.64 dB	$C/N(dB)=C/N0-BW$	
C/ACI,total	196.99 dB	$C/ACI^-1=C/ACIu^-1+C/ACId^-1$	
C/ASI,total	23.99 dB	$C/ASI^-1=C/ASIU^-1+C/ASId^-1$	
C/XPI,total	29.99 dB	$C/XPI^-1=C/XPIu^-1+C/XPI d^-1$	
C/IM,total	40.00 dB	$C/IM^-1=C/IMu^-1+C/IMd^-1$	
C/I,total	22.93 dB	$C/I^-1=C/ACI^-1+C/ASI^-1+C/XPI^-1+C/IM^-1$	
C/(N+I),total=Es/N0	14.04 dB	$C/(N+I)^-1=C/N^-1+ C/ACI^-1+C/ASI^-1+C/XPI^-1+C/$	
	Requiremr	Margin	
Req. Es/N0 and Ma	7.45	6.59	
Req. C/N inc. NLD	8.41	5.63	
Req. OBO	0.33	0.33	
Req. Csatpurecar/N	8.74	5.96	
NLD	0.96		Iteration Step: 0.10 dB
EARTH STATION POWER REQUIREMENT			
Txp SFD (Effective)	-92.00 dBW/m2	User defined	
Txp PFD	-94.00 dBW/m2	$=SFD-IBO$	
Φ (PFD) carrier	-97.07 dBW/m2		
Required EIRP	66.03 dBW	$=PFD\ Carrier+10log(4\pi R^2)+Ant.\ Misp+Atm.\ Absp.$	
Antenna Gain	52.82 dBi		
Antenna Feed Flang	13.21 dBW	$=Req\ EIRP-Ant.\ Gain$	
Coupling/WG Loss	0.30 dB		
Required HPA Power	13.51 dBW	$=Antenna\ Flange\ Power+Coupling/WG\ loss$	
Required HPA Power	22.46 W		
Used HPA Power	13.51 dBW		
Used HPA Power	22.5 W	User defined (if exists) or iterated	

Table 7 Link Budget Calculation – Outputs 2/2

OUTPUT 2/2				
DOWNLINK				
Txp EIRP	53.00	dBW	<i>User defined</i>	
Txp OBO	0.66	dB	<i>User defined</i>	
Defined Carrier OBO	3.73	dB	$=Txp\ OBO+10\log(Txp\ BW/Carr\ BW)$	
Def. Carrier D/L EIRP	49.27	dBW	$=Txp\ EIRP - Def.\ Carr\ OBO$	
Carrier OBO	3.73	dB	$=Txp\ OBO+10\log(Txp\ BW/Carr\ BW)+(Req.\ EIRP-Tx\ EIRP)$	
Carrier D/L EIRP	49.27	dBW	$=Txp\ EIRP - Carr\ OBO$	
Antenna Mispnt	0.30	dB	<i>User defined</i>	
L free space	205.52	dB	$L=(4.\pi.R/\lambda)^2$	
Atmospheric absorptic	0.09	dB	<i>Parameters table</i>	
Tlnb	58.66	°K	$Noise\ Temp=(NF-1)*290$	
Tsys	115.34	°K	$Tsys=Ta/Lfrx+Tf(1-1/Lfrx)+Tlnb$	
Tsys	20.62	dBK		
G/T	14.76	dB/K	$G/T=Gain-Lfrx-Tsys$	
C/N0d,thermal	86.72	dB/Hz	$C/N0u(dB)=EIRP-L+G/T-k$	
C/Nd,thermal	15.01	dB	$C/N(dB)=C/N0-BW$	
C/(N+I)d,thermal	14.68	dB	$C/(N+I)^{-1}=C/Nd^{-1}+ C/ACI^{-1}+C/ASI^{-1}+C/XPI^{-1}+C/IM^{-1}$	
Φ (PFD) carrier	-113.31	dBW/m2	$\Phi=EIRP-Ant.\ Misp-Atm.\ Abs.-10\log(4.\pi.R^2)$	
Rx Antenna Gain	35.68	dB		
P Rx @ Rx Ant	-120.96	dBW	$P\ Rx=EIRP-Ant.\ Misp-Atm.\ Abs-L\ free\ space+G\ Rx$	
CARRIER				
Carrier SR	14.80	MSymb/s		
Roll Off	0.20			
Carrier BW	17.76	MHz		
Info Rate Eff.	1.28	bps/Hz		
Info Rate (based on al	22.73	Mbps		
Info Rate (given roll of	22.73	Mbps		
% Txp BW Used	49%			
Used Carrier Power	49.27	dBW		
Defined Carrier Power	49.27	dBW		
Txp. EIRP - OBO	52.34	dBW		
% Txp Power Used	49%			
Power Eq. BW Used	18	MHz		
GENERAL				
	UP	DOWN		
C	40.79	40.79	°	
R	37567	37567	Km	
Elevation	42.85	42.85	°	
Azimuth	165.88	165.88	°	
Wavelength	0.0214	0.0250	m	$\lambda=c/f$
Antenna Gain	52.82	35.68	dBi	$G=Antenna\ Efficiency*(\pi\ d/\lambda)^2$
Half Power Beamwidth	0.405	2.917	°	$\Theta_{3dB}=k*\lambda/d=70*\lambda/d$

APPENDIX B

SIMULATION OUTPUT EXAMPLES

1. Single Carrier

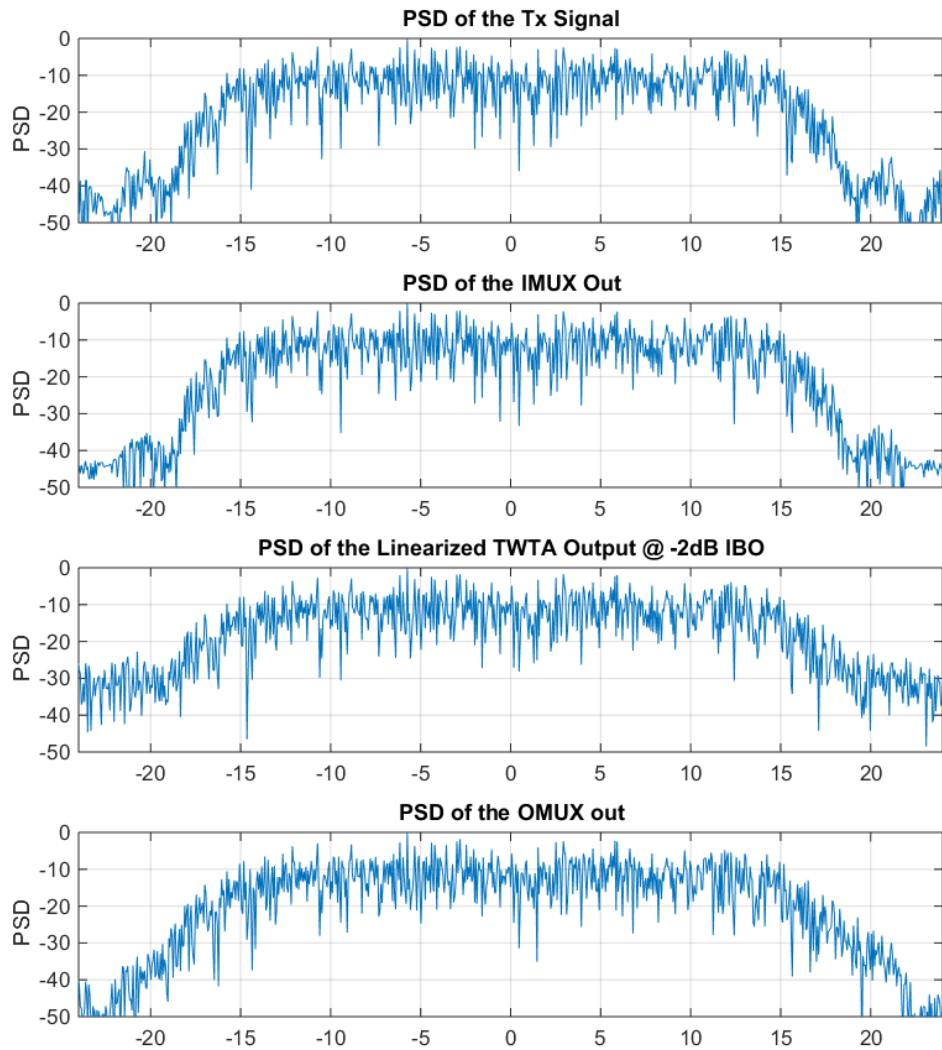


Figure 32 Power Spectral Density Plots of Single Carrier, LTWT at -2dB IBO

2. Dual Carrier

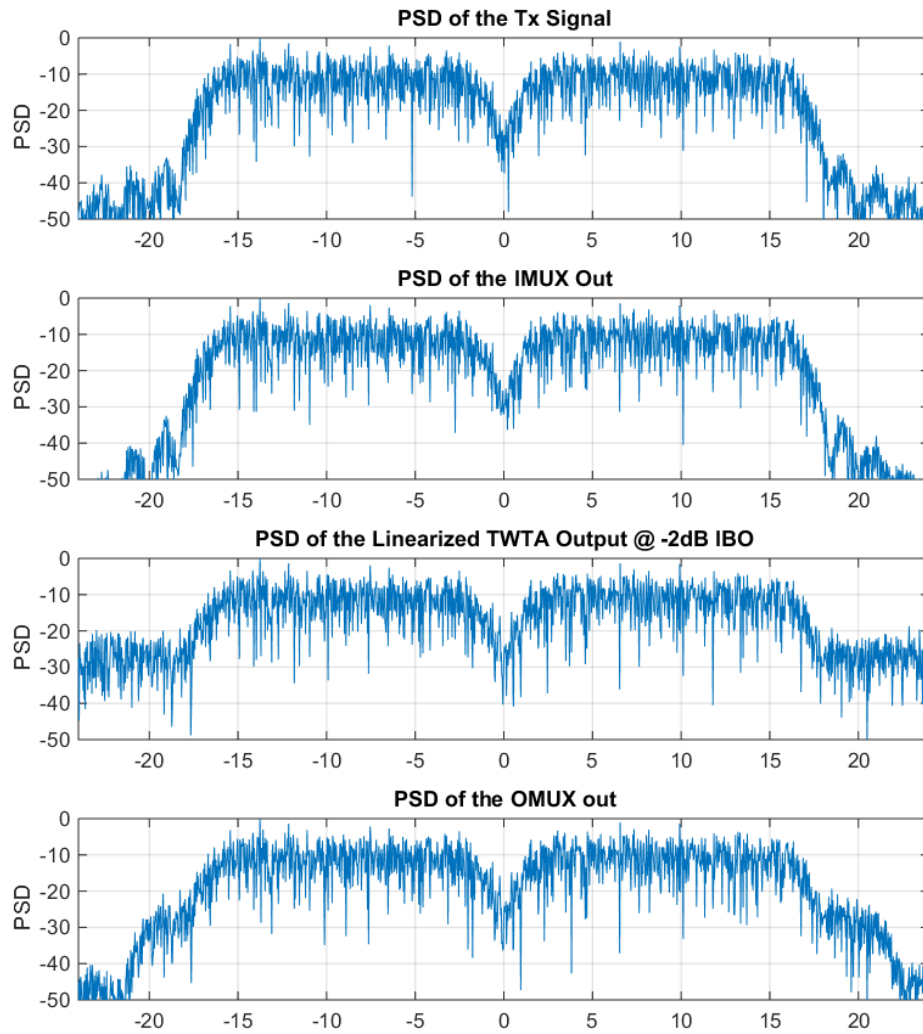


Figure 33 Power Spectral Density Plots of Dual Carriers, LTWT at -2dB IBO

3. 8 Carriers

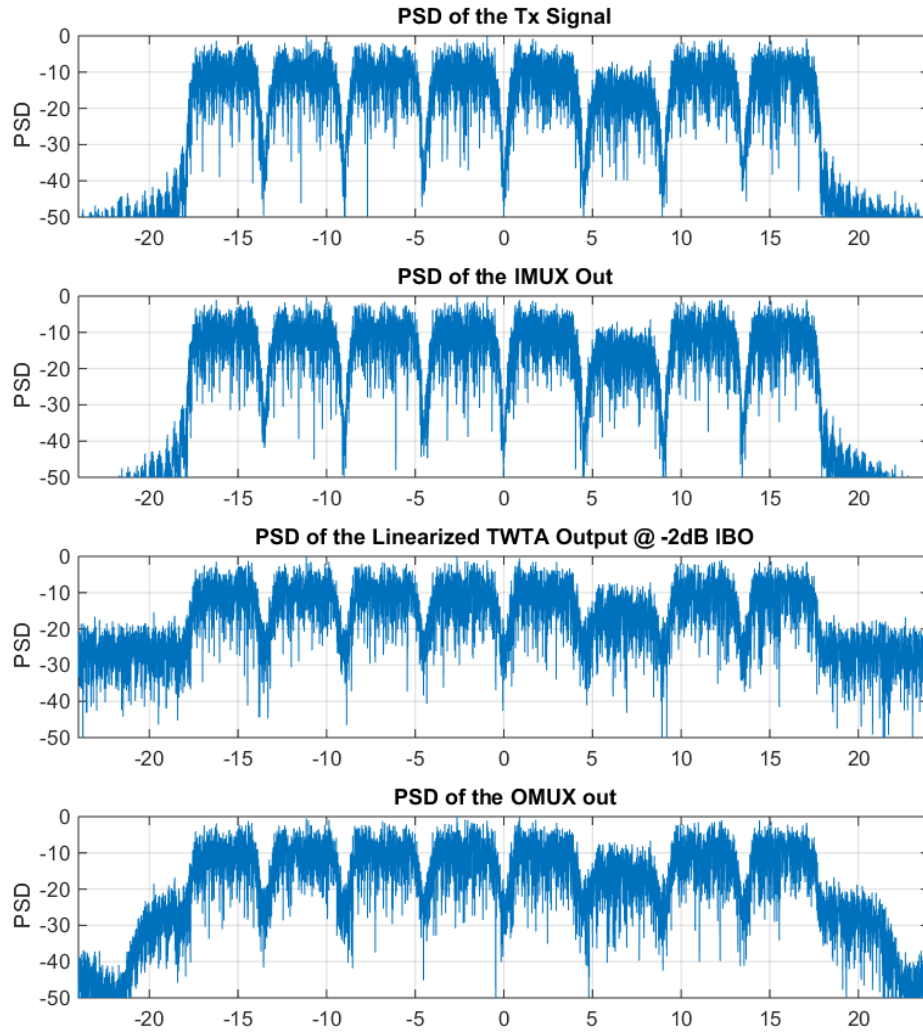


Figure 34 Power Spectral Density Plots of 8 Carriers, LTWT at -2dB IBO